1978

Bearing Capacity of Eccentrically Loaded Surface Footings on a Sand Layer Resting on a Rough Rigid Base

Roland Dale Maynard

BEARING CAPACITY OF ECCENTRICALLY LOADED SURFACE FOOTINGS ON A SAND LAYER RESTING ON A ROUGH RIGID BASE

By

Roland Dale Maynard

A thesis submitted
in partial fulfillment of the requirements for the
degree Master of Science, Major in
Engineering, South Dakota
State University
1978

BEARING CAPACITY OF ECCENTRICALLY LOADED SURFACE FOOTINGS ON A SAND LAYER RESTING ON A ROUGH RIGID BASE

This thesis is approved as a creditable and independent investigation by a candidate for the degree Master of Science, and is acceptable as meeting the thesis requirements for this degree, but without implying that the conclusions reached by the candidate are necessarily the conclusion of the major department.

Dr. Braja M. Das, Major Department Advisor — Date

Dr. Anwar S. Khattak, Major Department Assist. Advisor — Date

Prof. Emory E. Johnson, Head Civil Engineering Department — Date

ACKNOWLEDGEMENTS

I would like to express my greatest graditude to my advisor, Dr. Braja M. Das. Without his encouragement and selection of a thesis topic, my graduate studies could not have been completed. I would also like to express my personal admiration and respect for Dr. Das.

I would like to thank Dr. Awar Khattak for his valuable help and understanding through my last semester of graduate study.

Thanks also goes out to Prof. Emory E. Johnson. If not for the financial support received through Prof. Johnson, my graduate studies would not have been possible.

Thanks go to Mr. Alvin Biggar, Technical Assistant, for his help in the construction of the model test equipment.

A very special thanks goes to my wife, Nancy. If not for her understanding, encouragement and love, I would not have made it through my graduate studies.

RDM

NOTATIONS

$a_\theta = e^{(3/4 - \frac{\phi}{2})\tan\phi}$

$2B$ = width of footing

$2B'$ = effective width of footing

c = cohesion of soil

C_a = cohesive force

C_u = coefficient of uniformity

D_1, D_2 = maximum depth from ground surface down to where the slip surfaces will extend

e = eccentricity

G_s = specific gravity

H = depth of rigid base as measured from the base of the footing

Kpc, Kpq, Kp_γ = pure numbers whose values depend on the soil friction angle

L = length of footing

Nc, Nq, N_γ = bearing capacity factors

Nc', Nq', N_γ' = modified bearing capacity factors

P_p = Rankine passive pressure

Q = vertical load applied to the footing

q = uniform surcharge per unit area

q = load per unit area of the footing

q_u = ultimate load per unit area of the footing

r = radius at any point on a logarithmic spiral

r_o = initial radius on a logarithmic spiral

S = settlement

s = shear strength of soil

W = weight

δ = angle P_p makes with the normal line

γ = effective unit weight of soil

$\gamma_d(max.)$ = maximum dry density

$\gamma_d(min.)$ = minimum dry density

ϕ = internal angle of friction in soil

μ = angle sides of soil wedge makes with the horizontal

σ = normal stress

Θ = angle between r_o and any other radial line

TABLE OF CONTENTS

LIST OF ILLUSTRATIONS

LIST OF TABLES

CHAPTER I

INTRODUCTION

The foundation of a structure is defined as the lowest part of a structure. The function of this foundation is to transmit the weight of the structure onto the natural soil strata. If the soil is over stressed it will cause shear failure of the soil, and this shear failure could cause excessive settlement. This excessive settlement might result in dangerous structural damage.

Depending on the type of structure and the soil conditions encountered, there are several different types of foundations used. A "spread" foundation is simply a load bearing wall or column which is widened to transmit the load over a larger area to increase the bearing capacity. A "mat" foundation is a single slab covering the soil over the entire area of the structure. Mat foundations are used when the low bearing capacity of a soil causes the size of spread footing to become too large, and therefore it is more economical to use a mat foundation. "Pile" and "Caisson" foundations are used when the load transmitted from the structure is too large for the upper strata of soil, and the load has to be transmitted to the material located at greater depths.

Foundations are generally broken into two catagories. They are either classified as a shallow or as a deep foundation. Spread and mat foundations are classified as shallow foundations, where as pile and caisson foundations are classified as deep foundations. In 1943 Terzaghi defined quantitatively the difference between shallow and deep foundations. Using "D_f" as the vertical distance between the base of the footing and the ground surface, and "2B" as the width of the footing (see Figure 2.1), Terzaghi decided that if $2B \geq D_f$ this would be classified as a shallow foundation. If $2B < D_f$ the foundation would be classified as a deep foundation. In this paper I will be interested only with shallow foundations.

The ultimate bearing capacity of a shallow foundation is defined as the maximum load carrying capacity of a soil per unit area. Beyond this load the soil will undergo shear failure.

Prandlt in 1921 published results from his studies on the penetration of hard bodies into a softer material under the assumption of plastic equilibrium. Prandlt assumed the softer material to be homogeneous and isotropic. In 1943 Terzaghi furthered Prandlt's experiments for the study of ultimate bearing capacities for shallow foundations. Since that time numerous investigators such as Meyerhof (1943),

(1951), Caquot and Kerisel (1953), and Lundgren and Mortensen (1953), have refined the analysis introduced by Terzaghi.

Although there have been many intensive investigations run since the original investigations made by Terzaghi on shallow foundations, there are still aspects relating to the ultimate bearing capacity of shallow foundations that have yet to be studied extensively. One of these aspects is the bearing capacity of a foundation with a rigid base located at a shallow depth as measured from the base of the footing. Mandel and Salencon (1969), presented a theoretical analysis for ultimate bearing capacity of a foundation with a rigid base loacated at a shallow depth. Since that time there has been a limited number of investigations to verify Mandel and Salencon's theory. Tests under these conditions have been run by Meyerhof (1974) and Pfeifle (1978).

Another aspect that there has been limited research performed on is the ultimate bearing capacity of eccentrically loaded foundations. Meyerhof (1953) developed an empirical concept by which an eccentrically loaded footing may be regarded as a centrally loaded footing of reduced width (2B - 2e), in which "2B" equals the width of the footing and "e" equals the load eccentricity. DeBeer (1960) pointed out that Meyerhof's method gives a good estimate of bearing capacity for the eccentrically loaded footing.

There have also been tests run by Eastwood (1955), Ramelot and Vandeperre (1950), and Lee (1965) to confirm the results reached by Meyerhof.

The purpose of this investigation is to present the results of some recent laboratory model testing of the ultimate load carrying capacity of eccentrically loaded strip, surface footings on sand, with a rigid base located at varying depths. It is expected that these results will lend to a better quantatative understanding of the problems encountered in these situations.

CHAPTER II

REVIEW OF PAST WORK

2.1 Terzaghi's bearing capacity for shallow foundations

In explaining his bearing capacity theory, Terzaghi used a footing of width "2B" located at a depth "D_f" as shown in Figure (2.1).

For shallow foundations where $2B > D_f$ we can neglect the shearing resistance of the soil located above the level of the base of the footing. With this assumption we can replace this soil with unit weight "γ", by a surcharge $q = \gamma D_f$. If q_u is the ultimate load per unit area of the footing applied to cause failure, then the state of plastic equilibrium caused by this load q_u can be illustrated as shown in Figure (2.2).

The triangular area abe, marked as Zone I is an elastic zone. Terzaghi assumed that the sides ae and be of this zone rise at an angle to the horizontal of $\mu = \phi$. With q_u applied, this zone is pushed downward and thus pushing the soil masses in area aedc and befg laterally and upward. This causes the two areas aed and bef marked Zone II to become a zone of radial shear. The curves ed and ef are

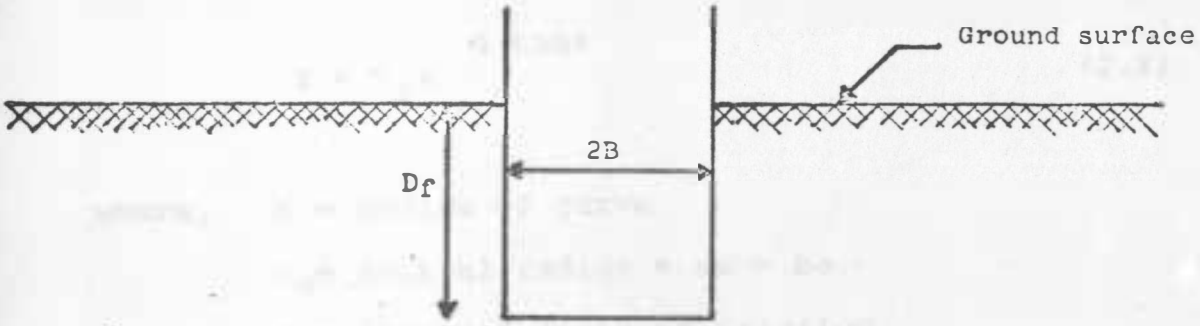

Figure 2.1 Stripfooting

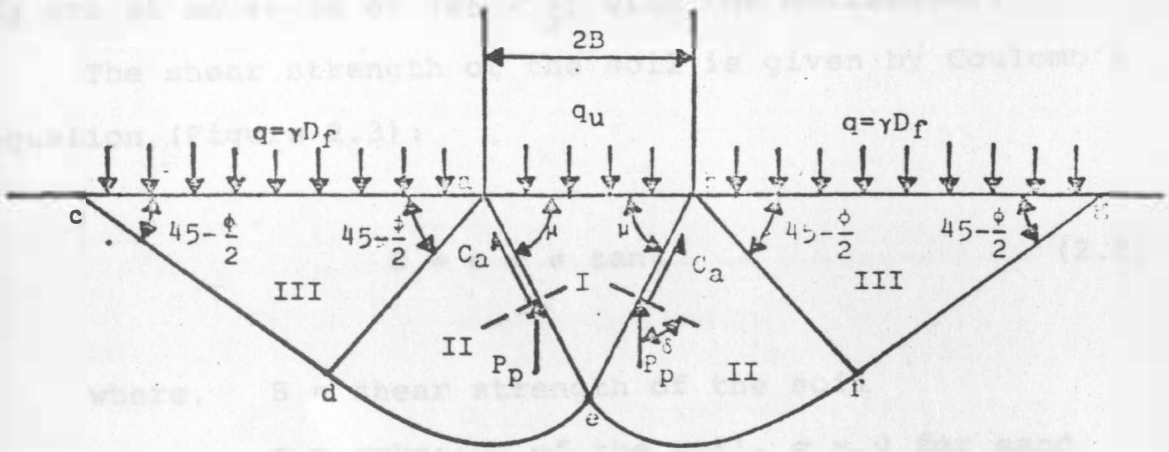

Figure 2.2 Terzaghi's bearing capacity analysis for rough stripfootings

assumed to be the arcs of a logarithimic spiral defined by the equation:

$$r = r_o e^{\theta \tan\phi} \qquad (2.1)$$

where, r = radius of curve

r_o = initial radius = ae = be

ϕ = internal angle of friction

θ = angle between r_o and any other radial line

The Zone marked III is a Rankine passive zone. The failure lines dc and fg are straight lines. Sides ad, cd, bf, and fg are at an angle of $(45 - \frac{\phi}{2})$ with the horizontal.

The shear strength of the soil is given by Coulomb's equation (Figure 2.3):

$$S = c + \sigma \tan\phi \qquad (2.2)$$

where, S = shear strength of the soil

c = cohesion of the soil, $c = 0$ for sand

σ = effective normal stress

ϕ = internal angle of friction

The ultimate bearing capacity can be calculated with the use of a free body diagram of wedge abe (Figure 2.4).

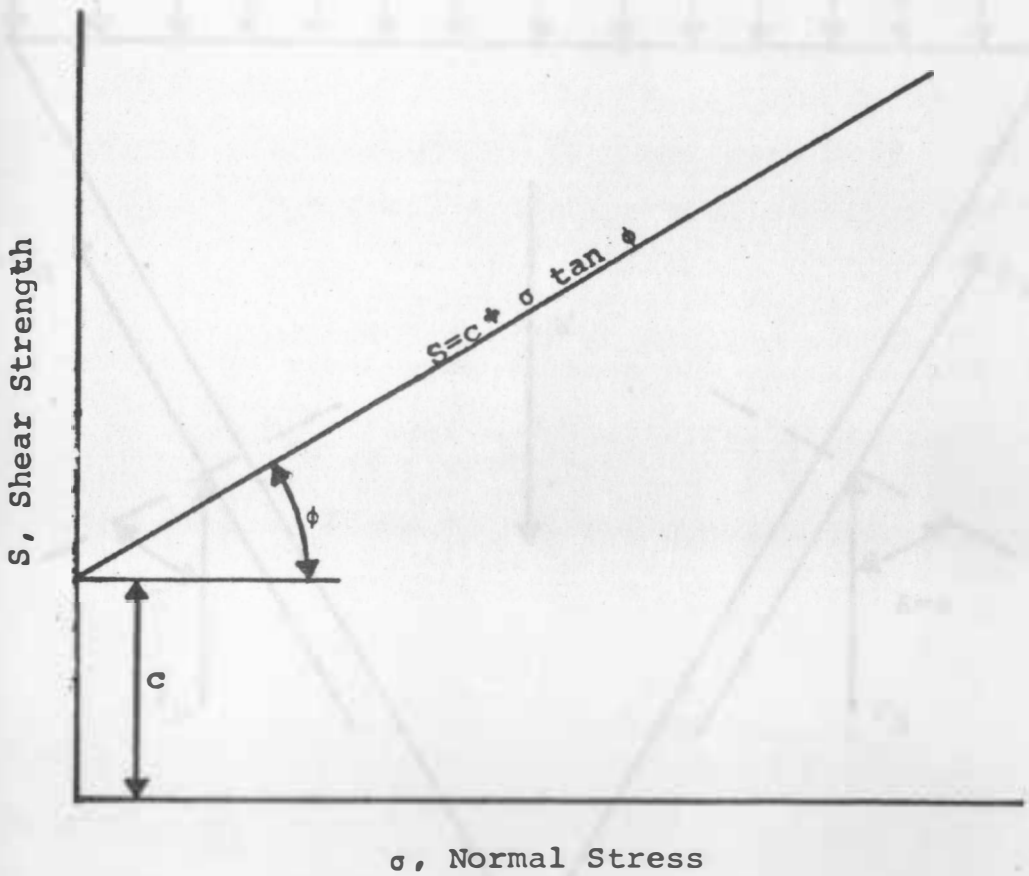

Figure 2.3 Shear strength of soil

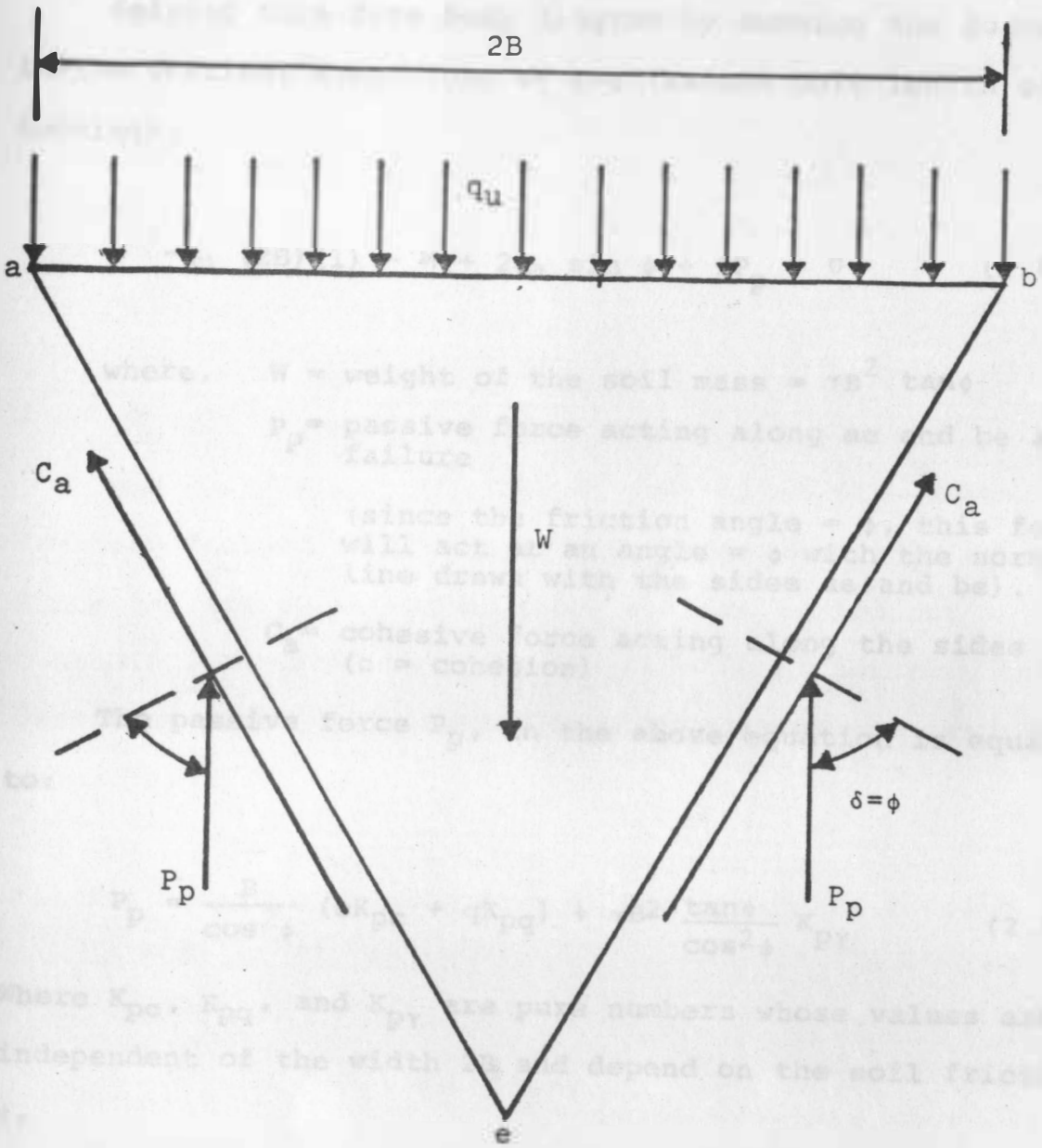

Figure 2.4 Free body diagram of soil wedge

Solving this free body diagram by summing the forces in the vertical direction, we get (assume unit length of the footing):

$$-q_u\ (2B)(1) - W + 2C_a \sin\phi + 2P_p = 0 \qquad (2.4)$$

where, W = weight of the soil mass = $\gamma B^2 \tan\phi$

P_p = passive force acting along ae and be at failure

(since the friction angle = ϕ, this force will act at an angle = ϕ with the normal line drawn with the sides ae and be).

C_a = cohesive force acting along the sides (c = cohesion)

The passive force P_p, in the above equation is equal to:

$$P_p = \frac{B}{\cos^2\phi}\ (cK_{pc} + qK_{pq}) + \gamma B^2\ \frac{\tan\phi}{\cos^2\phi}\ K_{p\gamma} \qquad (2.5)$$

Where K_{pc}, K_{pq}, and $K_{p\gamma}$ are pure numbers whose values are independent of the width 2B and depend on the soil friction, ϕ.

Substituting the values of P_p, W, and C_a into equation (2.4) and solving for q_u:

$$q_u = \gamma B\ (\tfrac{1}{2} \tan\phi\,(\frac{K_{p\gamma}}{\cos^2\phi} - 1) + c(\tan\phi + \frac{K_{pc}}{\cos^2\phi}) + q(\frac{K_{pq}}{\cos^2\phi}) \qquad (2.5)$$

where, $N_\gamma = \frac{1}{2} \tan\phi \left(\frac{K_{p\gamma}}{\cos^2\phi} - 1\right)$

$N_c = \tan\phi + \frac{K_{pc}}{\cos^2\phi}$

$N_q = \frac{K_{pq}}{\cos^2\phi}$

therefore,

$$q_u = \gamma B N_\gamma + c N_c + q N_q \qquad (2.6)$$

The coefficients N_γ, N_c, N_q are called the bearing capacity factors, with their values depending only on ϕ. Since the determination of these factors is tedious and time consuming, Terzaghi used the method of superposition to determine them. This method of superposition he used is shown below.

(1) for a grandular soil ($c = 0$) and a surface footing ($q = 0$) and ($\gamma \neq 0$):

$$q_u = \gamma B N_\gamma \qquad (2.7)$$

where, $N_\gamma = \frac{1}{2}\tan\phi \left(\frac{K_{p\gamma}}{\cos^2\phi} - 1\right)$

The values for $K_{p\gamma}$ are given in Table (2.1).

(2) For a weightless soil ($\gamma=0$) and a surface footing ($q=0$) and ($c\neq0$):

$$q_u = cN_c \tag{2.9}$$

where, $$N_c = \cot\phi \left(\frac{a_\theta^2}{2\cos^2(45+\frac{\phi}{2})} - 1\right) \tag{2.10}$$

$$a_\theta = e^{(3/4\,\pi - \frac{\phi}{2})\tan\phi} \tag{2.11}$$

(3) For a weightless soil ($\gamma=0$), no cohesion ($c=0$) and ($q\neq0$):

$$q_u = q\,Nq \tag{2.12}$$

where, $$Nq = \frac{a_\theta^2}{2\cos^2(45^o+\frac{\phi}{2})} \tag{2.13}$$

a_θ = same as above.

Even though the method of superposition is an approximate method, the answers obtained are on the safe side for evaluating the bearing capacity.

TABLE 2.1

VALUES FOR $K_{p\gamma}$ FOR ϕ=0 TO 50°

ϕ (deg)	$K_{p\gamma}$
0	10.8
5	12.2
10	14.4
15	18.6
20	25.0
25	35.0
30	52.0
35	82.0
40	141.0
45	298.0
50	800.0

2.2 Modifications to Terzaghi's bearing capacity theory

At the time that Terzaghi orginally formulated his bearing capacity theory, there had been a very limited amount of experimental results available. Since that time there has been extensive laboratory testing which has confirmed Terzaghi's assumption of the failure mechanism,

except that the angle μ, the angle ae and be make with the horizontal in the triangular section abe, is equal to a value between ϕ and $(45 + \frac{\phi}{2})$ that gives the minimum value for bearing capacity.

This new assumption changes the values of N_c, N_q, and N_γ. The ultimate bearing capacity for shallow foundations is still expressed in the form:

$$q_u = \gamma B N_\gamma + c N_c + q N_q \qquad (2.6)$$

Using the same method of superposition that Terzaghi used, the ultimate bearing capacity for a weightless soil ($\gamma = 0$) and a surface footing ($q = 0$) and ($c \neq 0$) can be given by:

$$q_u = c N_c \qquad (2.9)$$

In 1921 Prandlt introduced this value for N_c, under the assumption that $\mu = 45 + \frac{\phi}{2}$:

$$N_c = \cot\phi \; e^{\pi \tan\phi} \tan^2 (45 + \tfrac{\phi}{2}) - 1 \qquad (2.14)$$

A graph of Terzaghi's N_c and Prandlt's N_c vs. ϕ is shown in Figure (2.5). As can be seen from the graph, Prandlt's

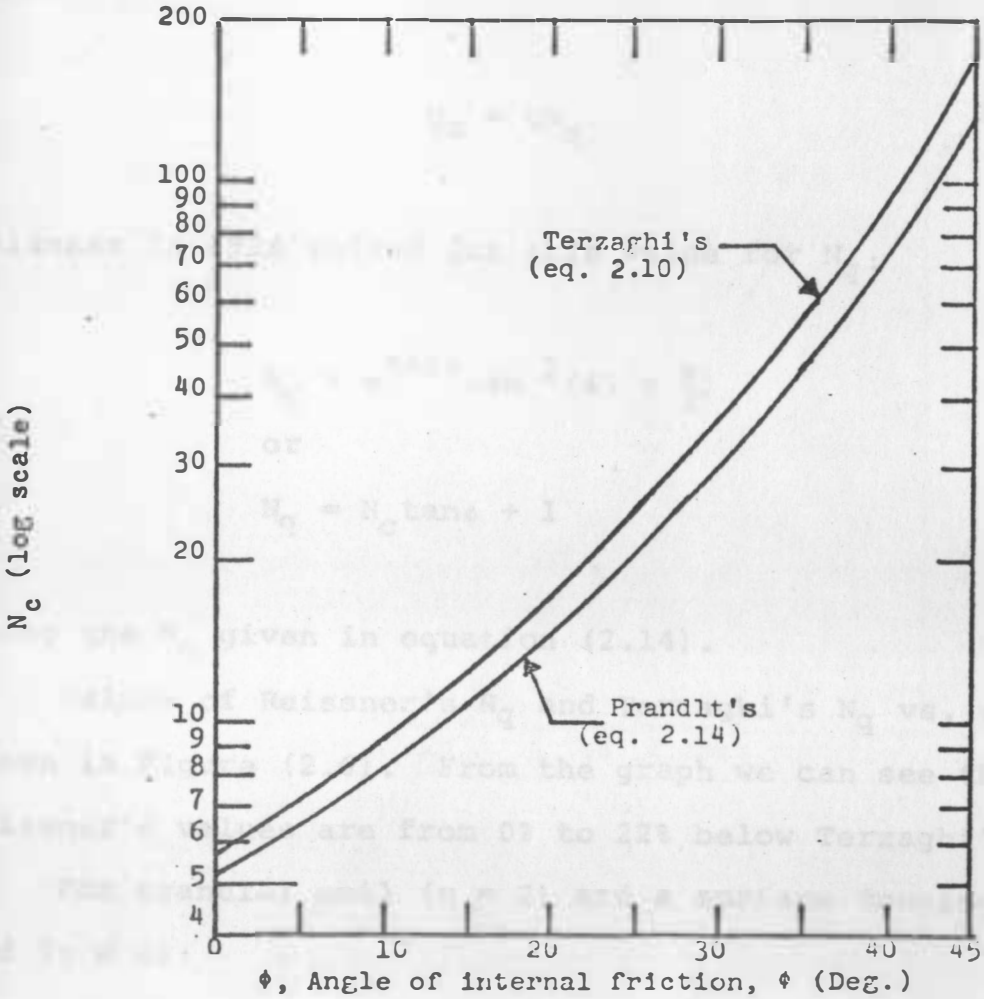

Figure 2.5 Comparison of Terzaghi's and Prandlt's values for N_c

values are from 10% to 23% lower than Terzaghi's values.

For a weightless soil ($\gamma = 0$), no cohesion ($c = 0$) and ($q \neq 0$):

$$q_u = qN_q \tag{2.12}$$

Reissner in 1924 solved for this value for N_q:

$$N_q = e^{\tan\phi} \tan^2\left(45 + \frac{\phi}{2}\right) \tag{2.15}$$

or

$$N_q = N_c \tan\phi + 1 \tag{2.15a}$$

Using the N_c given in equation (2.14).

Values of Reissner's N_q and Terzaghi's N_q vs. ϕ are shown in Figure (2.6). From the graph we can see that Reissner's values are from 0% to 22% below Terzaghi's.

For granular soil ($c = 0$) and a surface footing ($q = 0$) and ($\gamma \neq 0$):

$$q_u = \gamma B N_\gamma \tag{2.7}$$

Using Boussinesq's differential equation, Caquot and Kerisel (1953) gave values for N_γ. They found out that this factor varies sharply with the angle μ. Vesic (1973) showed that

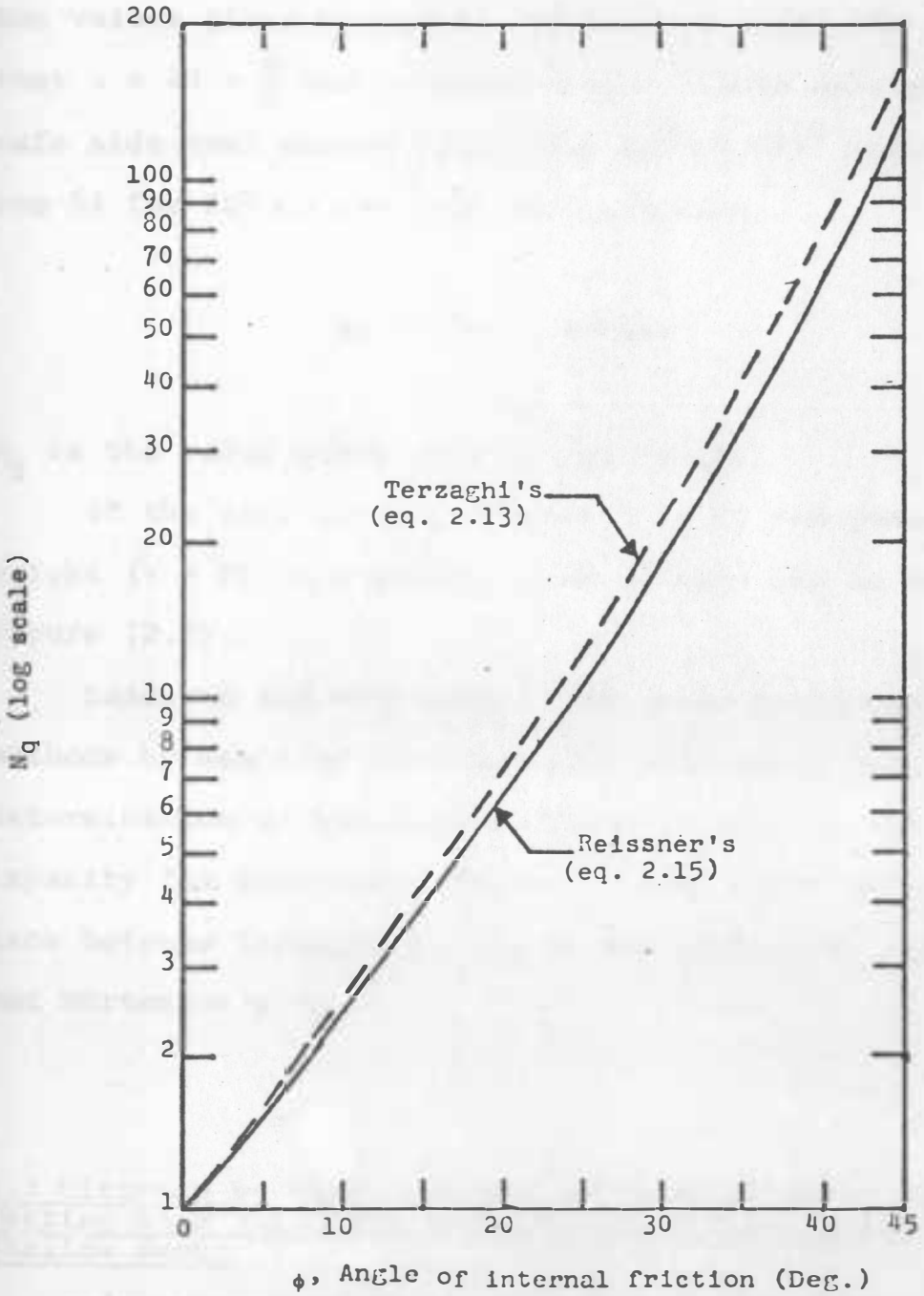

Figure 2.6 Comparison of Terzaghi's and Reissner's values of N_q

the values given by Caquot and Kerisel under the assumption that $\mu = 45 + \frac{\phi}{2}$ can be approximated within an error on the safe side (not exceeding 10% for $15^{o} < \phi < 45^{o}$ and not exceeding 5% for $20^{o} < \phi < 40^{o}$) by the equation:

$$N_{\gamma} = 2(N_q + 1)\tan\phi \qquad (2.16)$$

N_q is the value given by equation (2.15).

If the soil is cohesionless ($c = 0$) and possesses weight ($\gamma \neq 0$), the actual shear pattern may be shown as in Figure (2.7).

Lundgren and Mortensen (1953) have developed numerical methods by means of the theory of plasticity for the exact determination of the rupture lines as well as the bearing capacity for particular cases. Figure (2.9) shows a comparison between Terzaghi's, Caquot and Kerisel's, and Lundgren and Mortensen's N_{γ}.

2.3 Ultimate bearing capacity for a rough strip foundation resting on a soil with a rough, rigid base located at a shallow depth

Through use of the theory of limit equilibrium, Mandel and Salencon (1972) made a theoretical analysis for the ultimate bearing capacity of a rough, shallow, strip

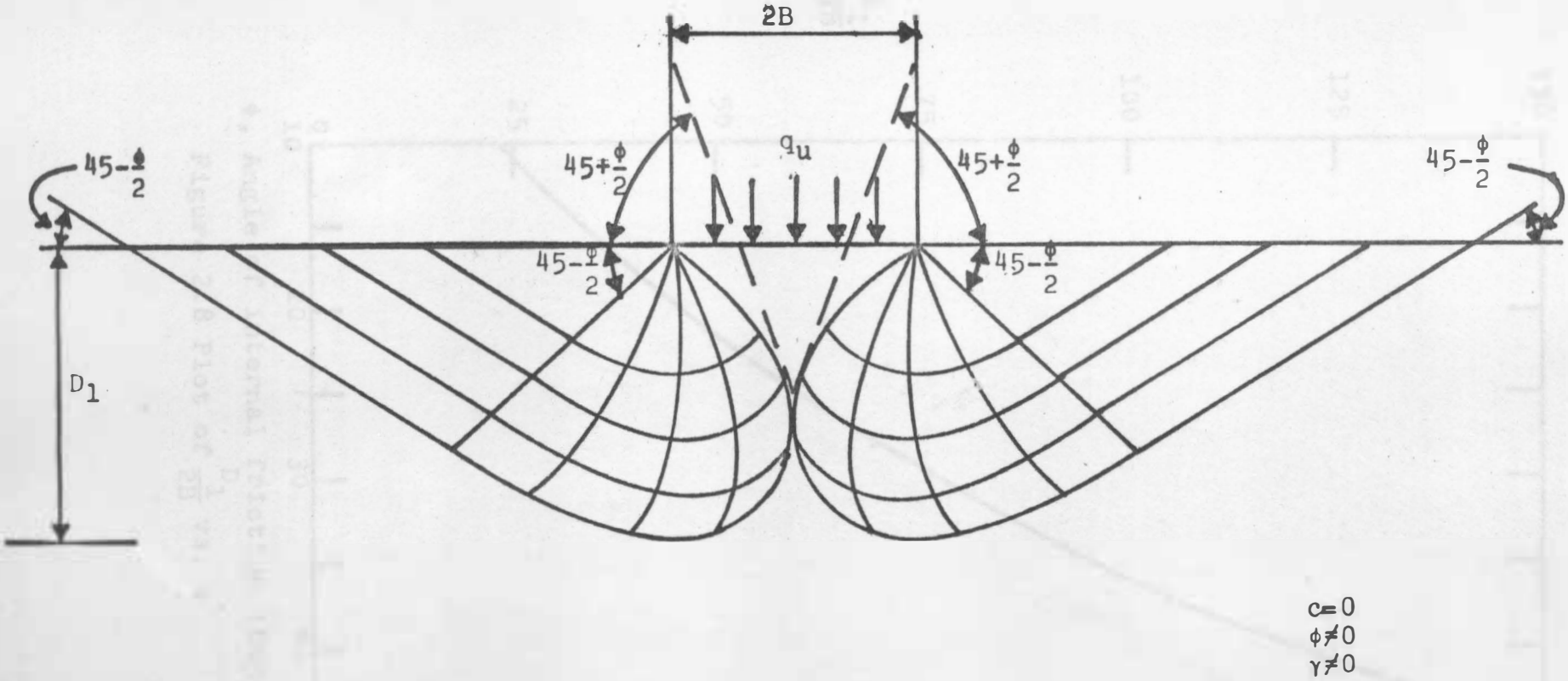

Figure 2.7 Shear pattern in soil for a rough surface footing

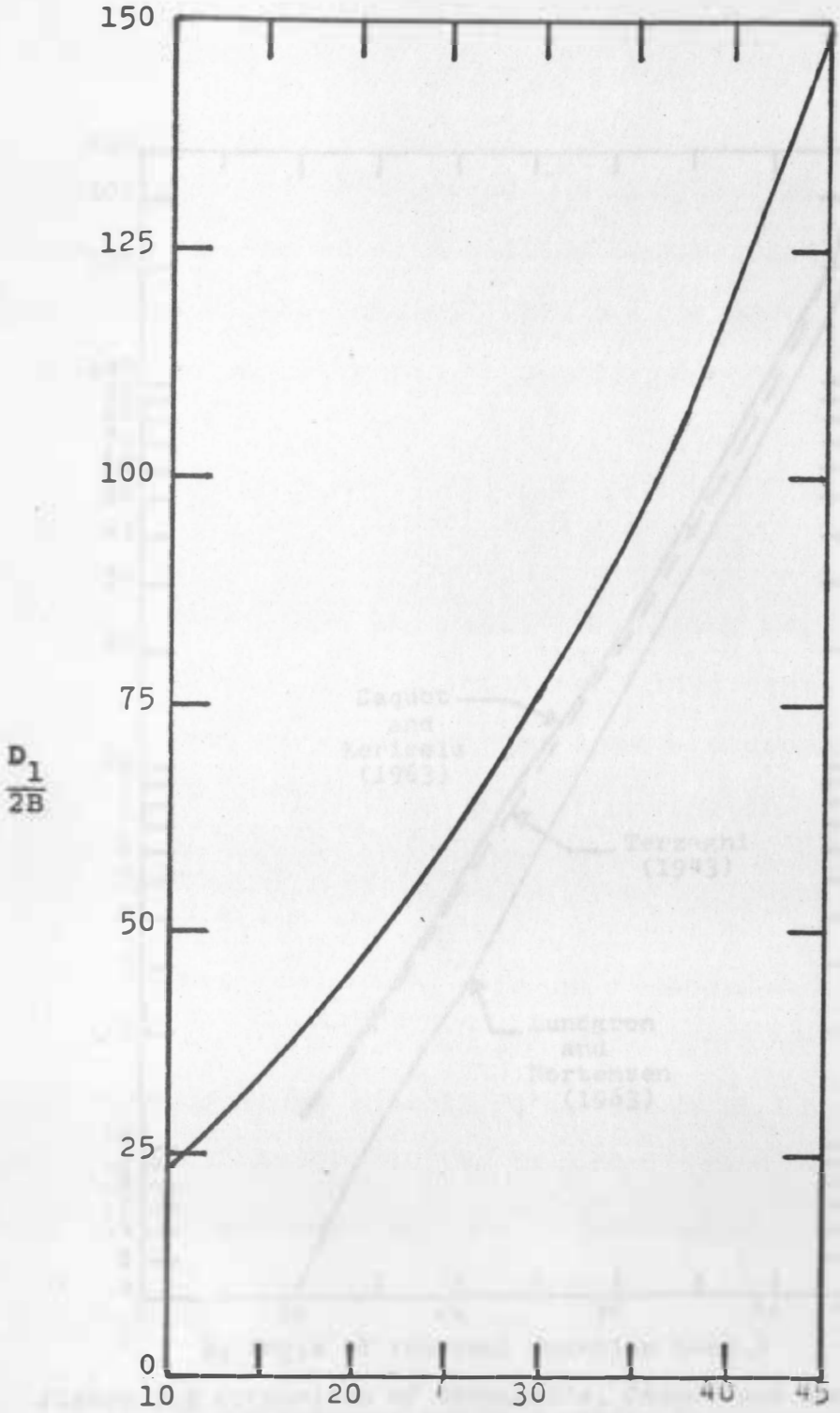

Figure 2.8 Plot of $\frac{D_1}{2B}$ vs. ϕ

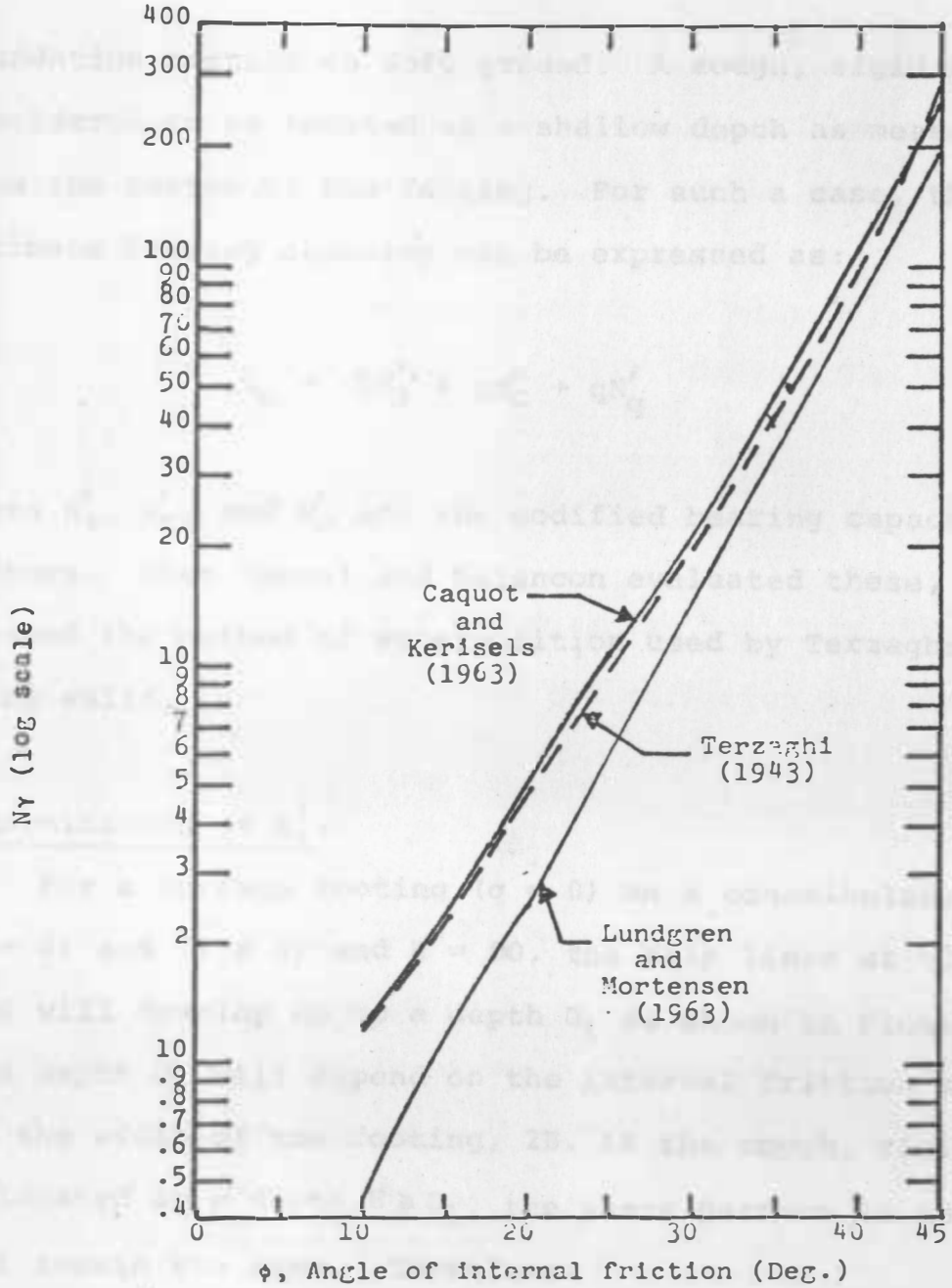

Figure 2.9 Comparison of Terzaghi's, Caquot and Kerisel's, and Lundgren and Mortensen's N_γ

foundation resting on soft ground. A rough, rigid base was considered to be located at a shallow depth as measured from the bottom of the footing. For such a case, the ultimate bearing capacity can be expressed as:

$$q_u = \gamma B N'_\gamma + c N'_c + q N'_q \qquad (2.17)$$

Where N'_γ, N'_c, and N'_q are the modified bearing capacity factors. When Mandel and Salencon evaluated these, they assumed the method of superposition used by Terzaghi as being valid.

Determination of N'_γ:

For a surface footing ($q = 0$) on a cohesionless soil ($c = 0$) and ($\gamma \neq 0$) and $H = \infty$, the slip lines at ultimate load will develop up to a depth D_1 as shown in Figure (2.7). This depth D_1 will depend on the internal friction angle ϕ, and the width of the footing, 2B. If the rough, rigid base is located at a depth $H \geq D_1$, the shear pattern in the soil will remain the same. Therefore:

$$q_u = \gamma B N'_\gamma \quad (\text{for } H \geq D_1) \qquad (2.18)$$

where, $N'_\gamma = N_\gamma$

Mandel and Salencon assumed that the Lundgren and Mortensen's N_γ is correct, therefore those values should be used in equation (2.18). Figure (2.8) shows a plot of $\frac{D_1}{2B}$ vs. the internal angle of friction, ϕ.

If $H < D_1$, the shear pattern of the soil supporting the foundation will change, thus N'_γ will change. For this case:

$$q_u = \gamma B N'_\gamma \quad (\text{for } H < D_2) \tag{2.19}$$

When $N'_\gamma > N_\gamma$ (Lundgren and Mortensen's) and is a function of $\frac{H}{2B}$ and ϕ. Figure (2.10) shows the variation of N'_γ with ϕ and $\frac{H}{2B}$.

Determination of N'_c:

In Figure (2.11a), a rigid base is located a depth, H. If H = ∞ the slip surface will occur as shown in Figure (2.11a) under q_u. If we assume a weightless soil ($\gamma = 0$), with a surface footing ($q = 0$) and ($c \neq 0$), the ultimate bearing capacity will be:

$$q_u = cN'_c \tag{2.20}$$

where, $N'_c = N_c$ (Prandlt's) (2.14)

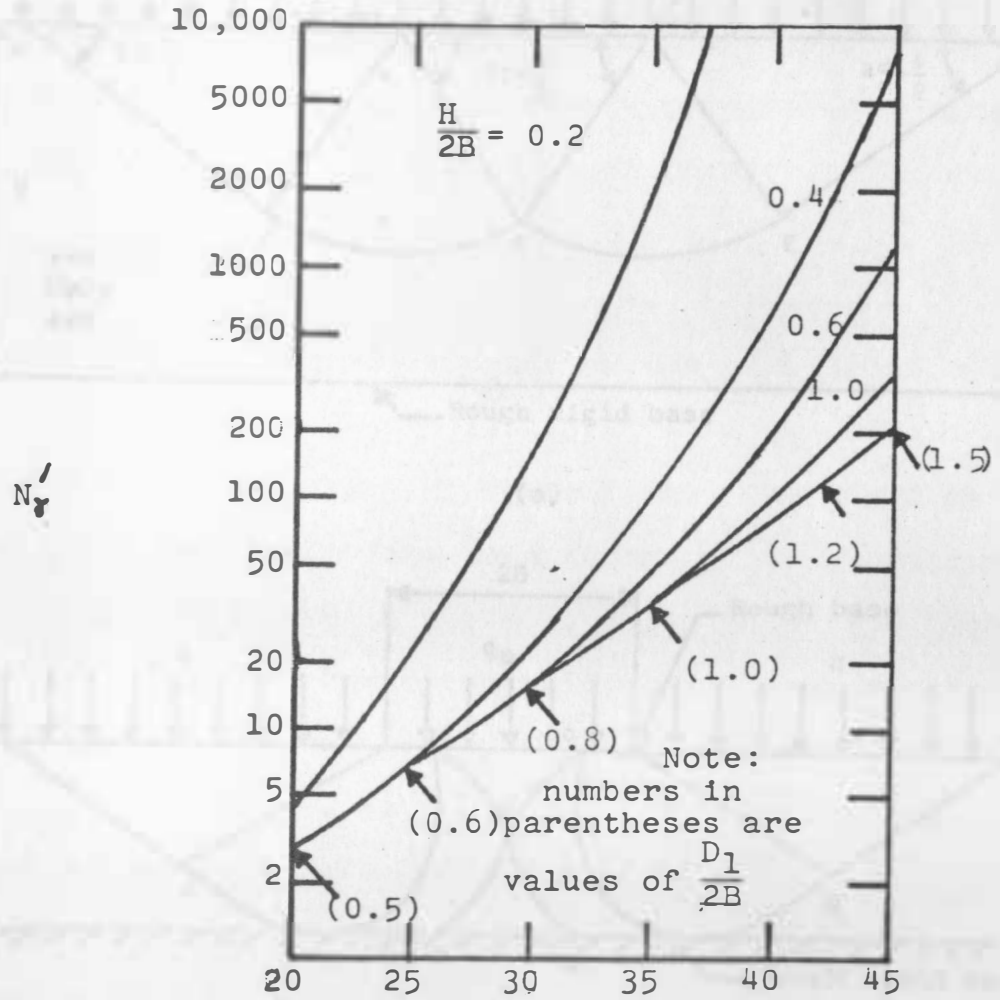

Figure 2.10 Plot of N_γ' vs. ϕ (after Meyerhof, 1974, from the numerical values of Mandel and Salencon).

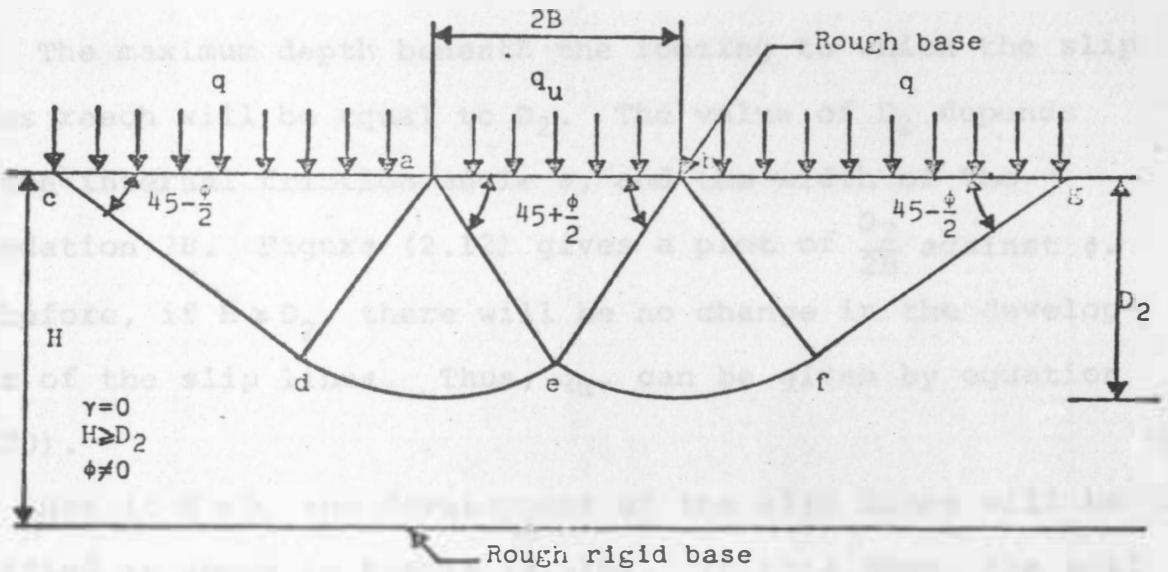

(a)

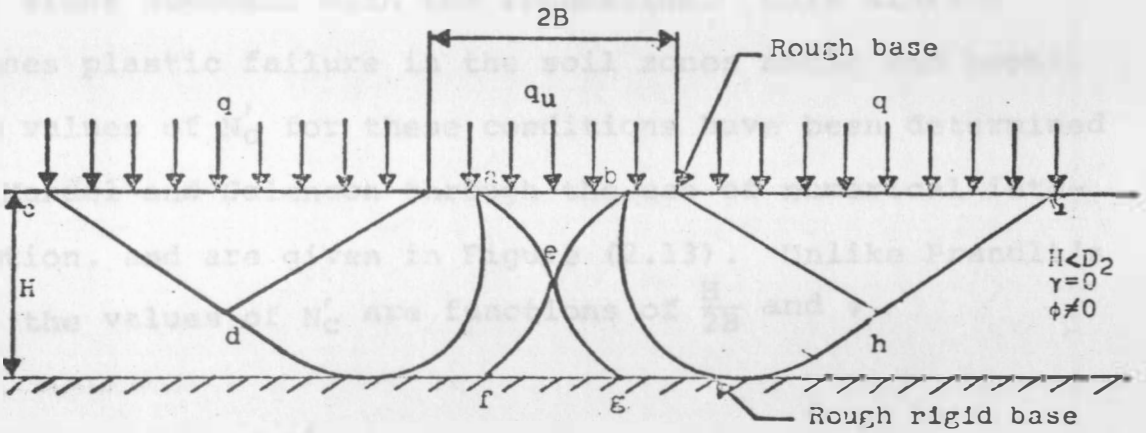

(b)

Figure 2.11 Effect of a rigid base on the slip surface of a soil.

The maximum depth beneath the footing to which the slip lines reach will be equal to D_2. The value of D_2 depends on the internal friction angle ϕ, and the width of the foundation 2B. Figure (2.12) gives a plot of $\frac{D_2}{2B}$ against ϕ. As before, if $H \geq D_2$, there will be no change in the development of the slip lines. Thus, q_u, can be given by equation (2.20).

But if $H < D_2$ the development of the slip lines will be modified as shown in Figure (2.11b). In this case, the soil mass in the zone efg remains motionless. The rigid wedge abe sinks downward with the foundation. This sinking causes plastic failure in the soil zones aefdc and beghi. The values of N'_c for these conditions have been determined by Mandel and Salencon through the use of numerical integration, and are given in Figure (2.13). Unlike Prandlt's N_c, the values of N'_c are functions of $\frac{H}{2B}$ and ϕ.

Determination of N'_q:

Referring to Figure (2.11a), if we assume ($\gamma = 0$), ($c = 0$), ($q \neq 0$), and that the rigid base is located at a depth $H = \infty$, then the slip lines will develop to a depth D_2 as measured from the bottom of the base. Therefore:

$$q_u = qN'_q \qquad (2.21)$$

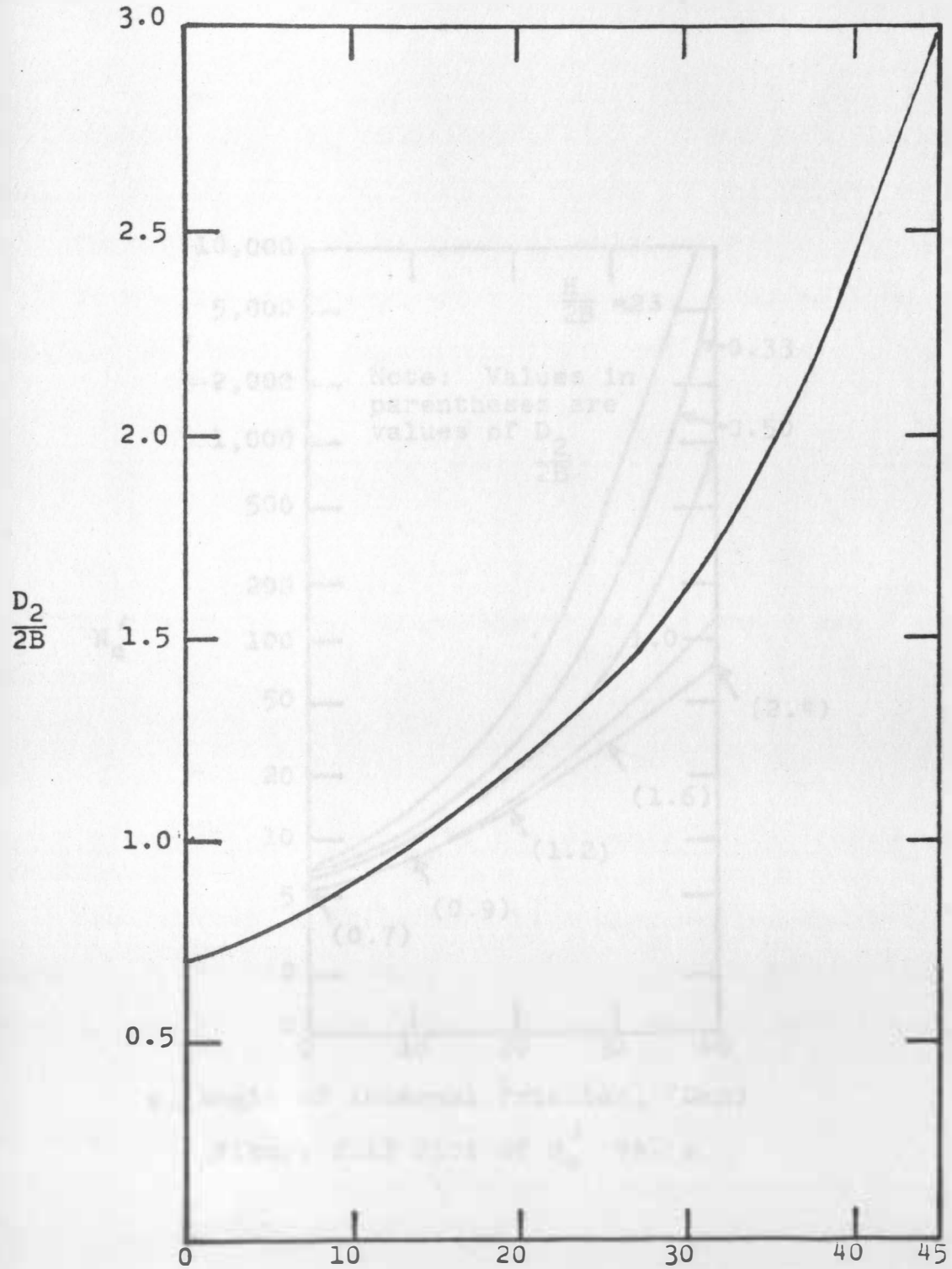

Figure 2.12 Plot of $\frac{D_2}{2B}$ vs. ϕ

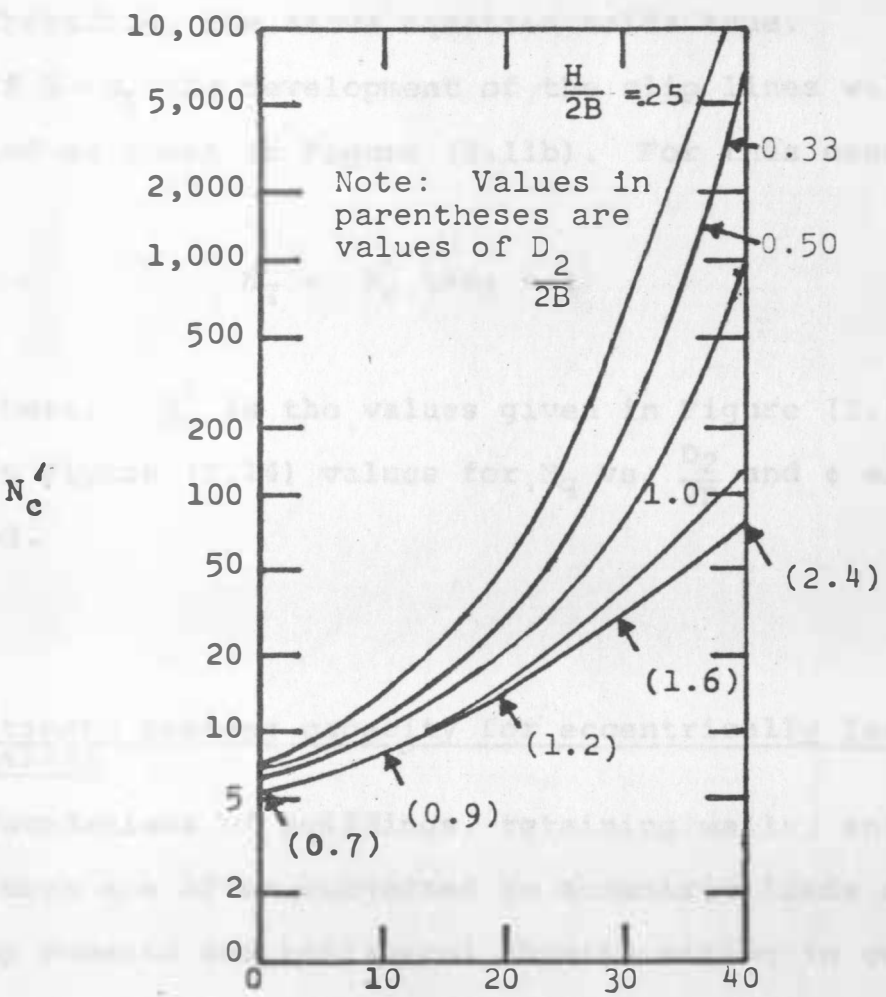

Figure 2.13 Plot of N_c' vs. ϕ

where, $N'_q = N_q$ (Reissner's) (2.15)

Again, if $H \geq D_2$ there will be no change in the values of N'_q. Therefore, the above equation holds true.

If $H < D_2$ the development of the slip lines will be modified as shown in Figure (2.11b). For this case

$$N'_q = N'_c \tan\phi + 1 \qquad (2.22)$$

where, N'_c is the values given in Figure (2.13).

In Figure (2.14) values for N'_q vs. $\frac{D_2}{2B}$ and ϕ are plotted.

2.4 Ultimate bearing capacity for eccentrically loaded foundations

Foundations of buildings, retaining walls, and similiar structures are often subjected to eccentric loads due to bending moments and horizontal thrusts acting in conjunction with the vertical loading. With this eccentric load applied, the contact pressures below the base of the footing are generally taken as to decrease linearly towards the heel from a maximum at the toe. But Meyerhof (1953) determined that for eccentrically loaded foundations at the ultimate bearing capacity, the distribution of contact pressure is not even approximately linear, and that a very simple

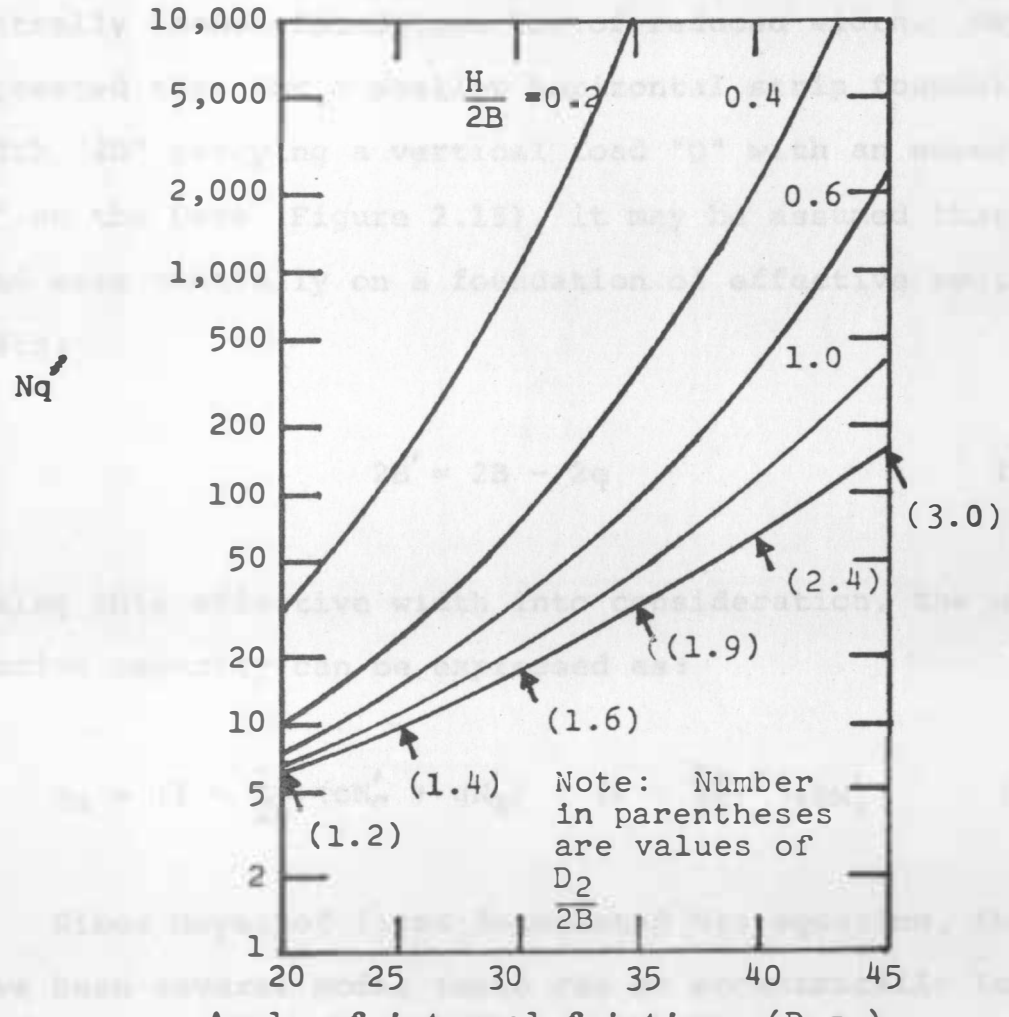

Figure 2.14 Plot of N_q' vs. ϕ

solution to the problem is obtained by assuming that the contact pressure distribution is identical to that for a centrally loaded foundation but of reduced width. Meyerhof suggested that for a shallow horizontal strip foundation of width "2B" carrying a vertical load "Q" with an eccentricity "e" on the base (Figure 2.15), it may be assumed that the load acts centrally on a foundation of effective contact width:

$$2B' = 2B - 2e \qquad (2.23)$$

Taking this effective width into consideration, the ultimate bearing capacity can be expressed as:

$$q_u = (1 - \frac{2e}{2B})(cN'_c + qN'_q) + (1 - \frac{2e}{2B})^2 \gamma B N'_\gamma \qquad (2.24)$$

Since Meyerhof first formulated his equation, there have been several model tests run on eccentrically loaded footing failures. Table (2.2) gives a summary of these tests.

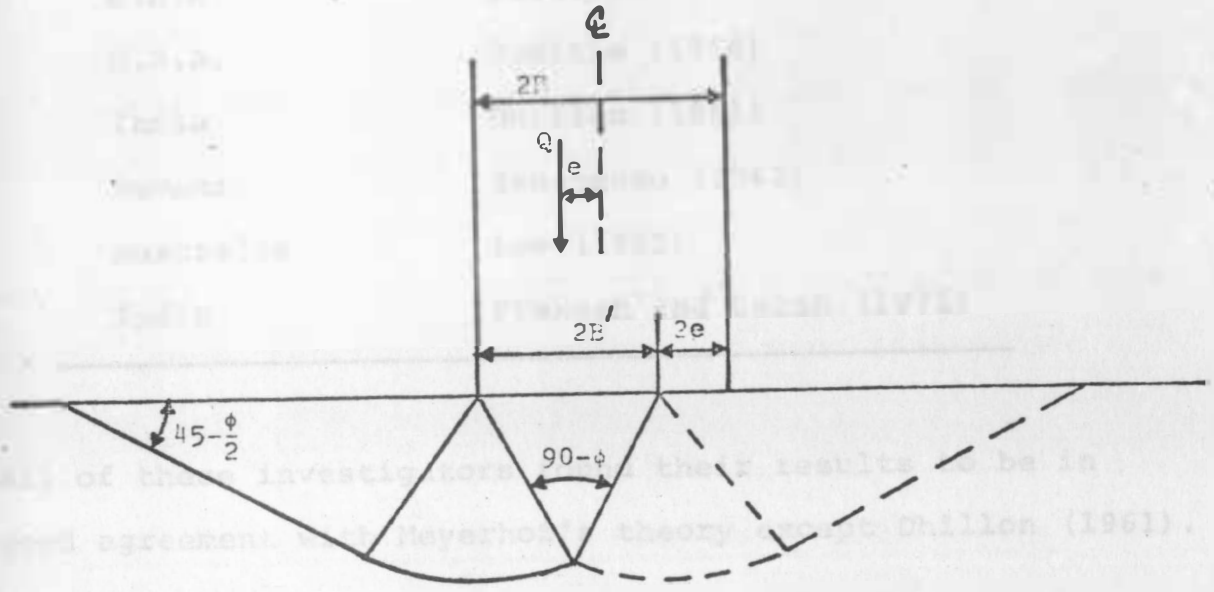

Figure 2.15 Eccentrically loaded footing(after Meyerhof (1953)).

TABLE 2.2

MODEL TESTS RUN ON ECCENTRICALLY LOADED FOOTINGS

Country	Investigator
U.S.A.	Eastwood (1955)
U.S.A.	Jumikis (1956)
India	Dhillon (1961)
Rumania	Zaharescu (1961)
Australia	Lee (1965)
India	Prakash and Saran (1971)

All of these investigators found their results to be in good agreement with Meyerhof's theory except Dhillon (1961).

CHAPTER III

LABORATORY MODEL TESTS

3.1 General

Small scale tests were run in the laboratory to study the effects on the ultimate bearing capacity of eccentrically loaded rough, strip, shallow foundations due to a rigid base located at varying depths. The settlement of the footing was also observed. The eccentricity of the load was varied from e = 0", to e = 1.5" on a footing 4" x 12". All the model tests in this experiment were limited to surface footings on cohesionless soil.

3.2 Physical properties of the sand used in the tests

As was mentioned above, sand was used in all of the tests run. The sand used was an Ottawa CN-501 density sand.

Standard tests were run on the sand to determine the significant properties of the soil. The properties of the sand are given in Table (3.1). The grain-size distribution curve for the sand can be seen in Figure (3.1). From examination of the grain-size distribution curve one can see that this is an uniformly graded soil with little fine grains present.

TABLE 3.1

CHARACTERISTICS OF SAND USED FOR MODEL TEST

% Passing U.S. Sieve No. 20	100
% Passing U.S. Sieve No. 40	24.71
% Passing U.S. Sieve No. 60	4.90
% Passing U.S. Sieve No. 80	0.71
Angle of internal friction, ϕ	37^{o}
Coefficient of Uniformity, C_u	1.35
Specific Gravity, G_s	2.61
Maximum dry density , $\gamma_{d(max.)}$	108.28 pcf
Void Ratio at maximum density	.504
Minimum dry density, $\gamma_{d(min.)}$	95.95 pcf
Void Ratio at minimum density	.697

[1](pcf = 15.95 kg/m^3)

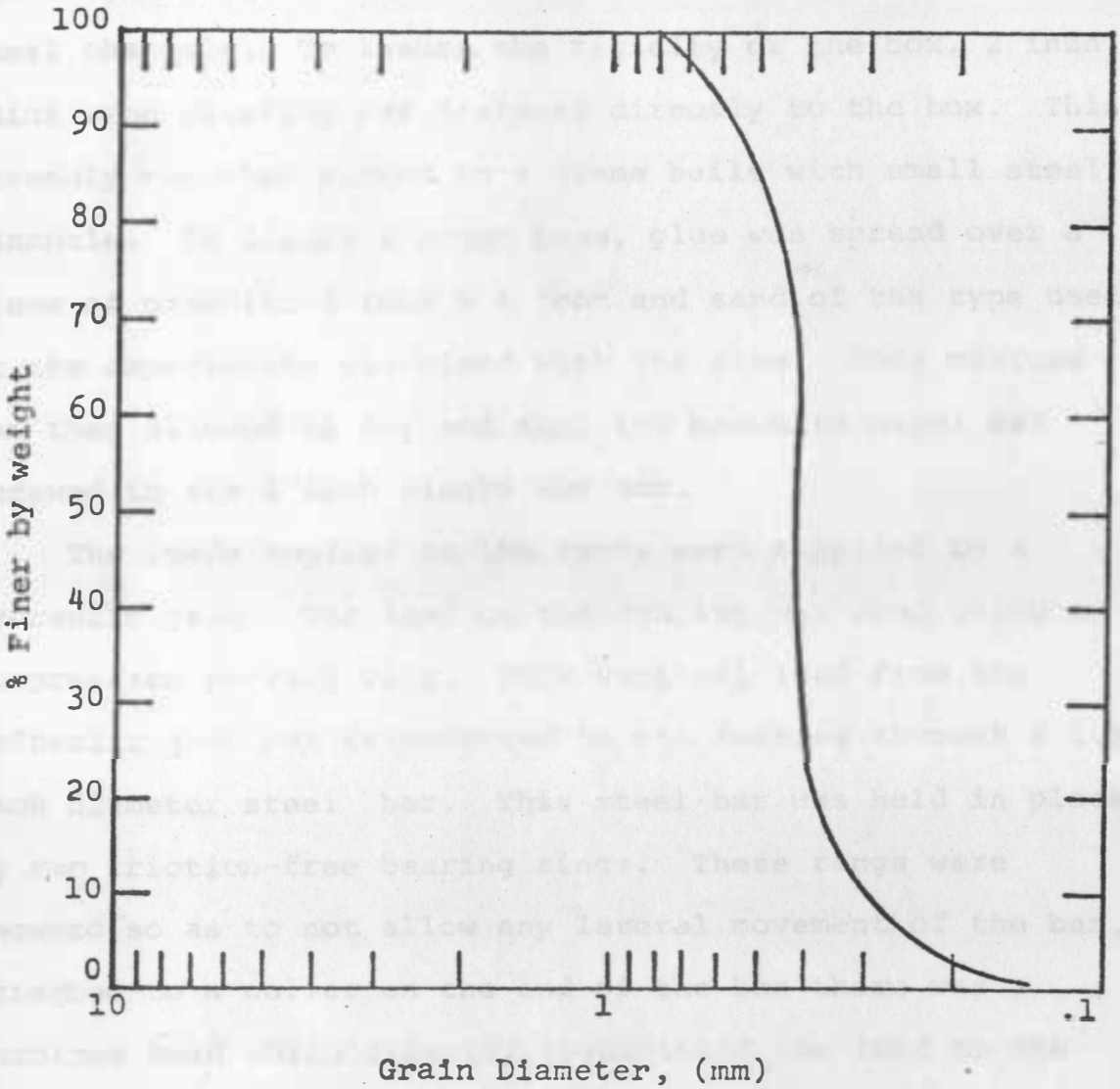

Figure 3.1 Grain size distribution curve

3.3 Description of Model Testing Equipment.

Tests were run in a box measuring 3 feet x 1 foot x 1.5 feet. The walls of the box were reinforced using small steel channels. To insure the rigidity of the box, 2 inch thick wood planking was fastened directly to the box. This assembly was then placed in a frame built with small steel channels. To insure a rough base, glue was spread over a piece of masonite 3 feet x 1 foot and sand of the type used in the experiments was mixed with the glue. This mixture was then allowed to dry and then the masonite panel was screwed to the 2 inch planks and box.

The loads applied on the tests were supplied by a hydraulic jack. The load on the footing was read using a compression proving ring. This vertical load from the hydraulic jack was transmitted to the footing through a 1.5 inch diameter steel bar. This steel bar was held in place by two friction-free bearing rings. These rings were located so as to not allow any lateral movement of the bar. Attached to a collar on the end of the box there was a machined head which directly transmitted the load to the footing through a roller bearing 3/8 inch diameter by 1 1/2 inch length. The general layout of the equipment used is shown in Figure (3.2).

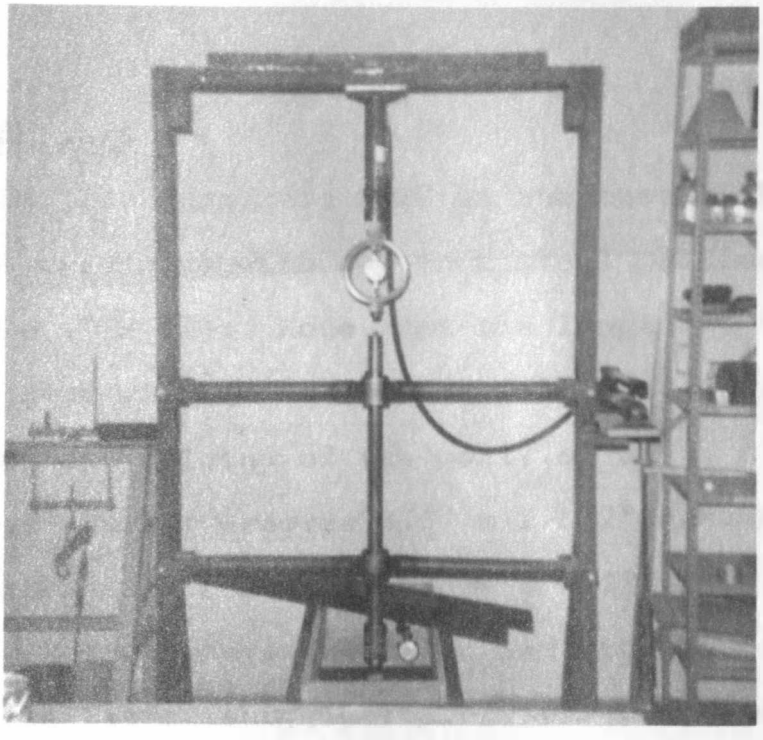

Fig. 3.2 General layout of model test equipment.

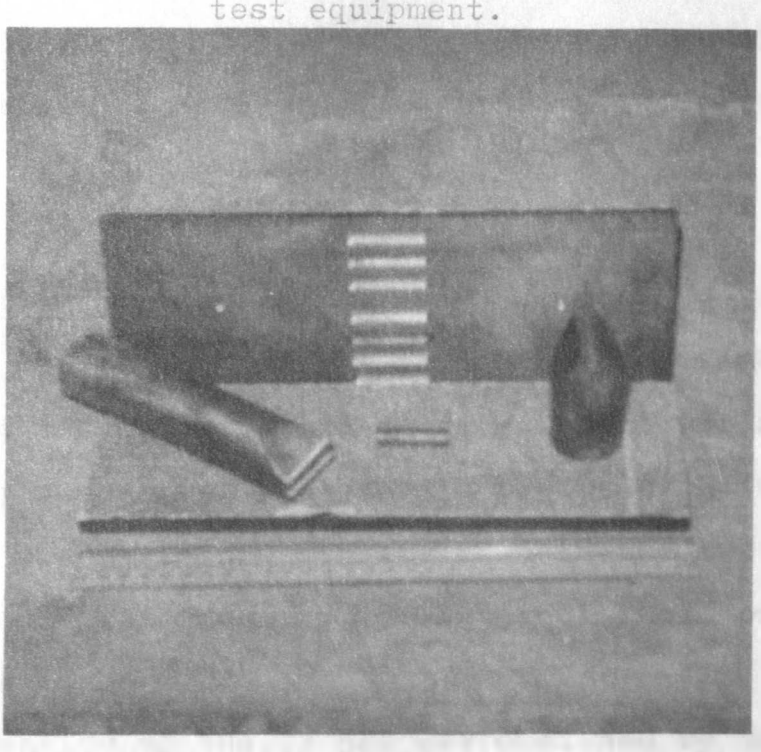

Fig. 3.3 Test footings used in model study.

3.4 Model footings

Two model footings were used in the tests. Each of these plates were made with 1/4 inch steel platings. Both footings were 4" x 12". Note that the length of the footings is the same width as the box. This identical length would prevent end bulging of the soil, so as to simulate a plain strain case. Grooves 3/8" x 1 1/2" were machined into the plates at eccentricities of e = 0", 1/2", 3/4", 1", and 1 1/2". These grooves were machined to size so that the roller bearing fitted snuggly in to them. Sand paper was glued to the underside of the footings so as to simulate a rough footing (Figure 3.3). Holes were also machined into the top of the plates in order to measure the settlement of the footing with a displacement dial.

3.5 Preparation and Testing

Before the tests could be performed, the sand had to be compacted to predetermined density. This was accomplished by uniformly compacting the sand in layers of 2 inches in depth. The predetermined density used in the test was 104.27 pcf. At this density the internal angle of fricition ϕ, was found to be 37^{o}.

This density of 104.27 pcf was obtained by uniformly compacting 53.135 pounds of the sand into a layer 2 inches

in depth. To measure this 2 inch thickness, lines were drawn around the inside of the box every 1 inch as measured from a static plane above the box. The sand was then placed in the box and compacted to the desired height. After the sand was compacted to the desired height, the footing was placed in the right position in the box gently so as to not transmit any extra load on the sand. Then a micrometer was placed, as shown in Figure (3.5), to measure the settlement of the footing. (Numerous tests were run with micrometers set up on both sides of the footing to check for tilting of the footing to one side or the other. From these tests there wasn't tilting in either direction to make a significant difference in the results of the tests.) Next a load was applied to the footing from the hydraulic jack. This load was applied and recorded for every .01 inch of settlement until the ultimate load was reached. From these readings load-settlements graphs were drawn.

After each test the surface failure pattern was observed, and in some cases photographs were taken of the failure patterns. Figure (3.5) shows the failure pattern for footing loaded with an eccentricity = 0". Figure (3.7) shows the failure pattern for a footing loaded with an eccentricity = 1.5". Notice the loss of contact between the soil and the base of the footing when the eccentricity = 1.5"

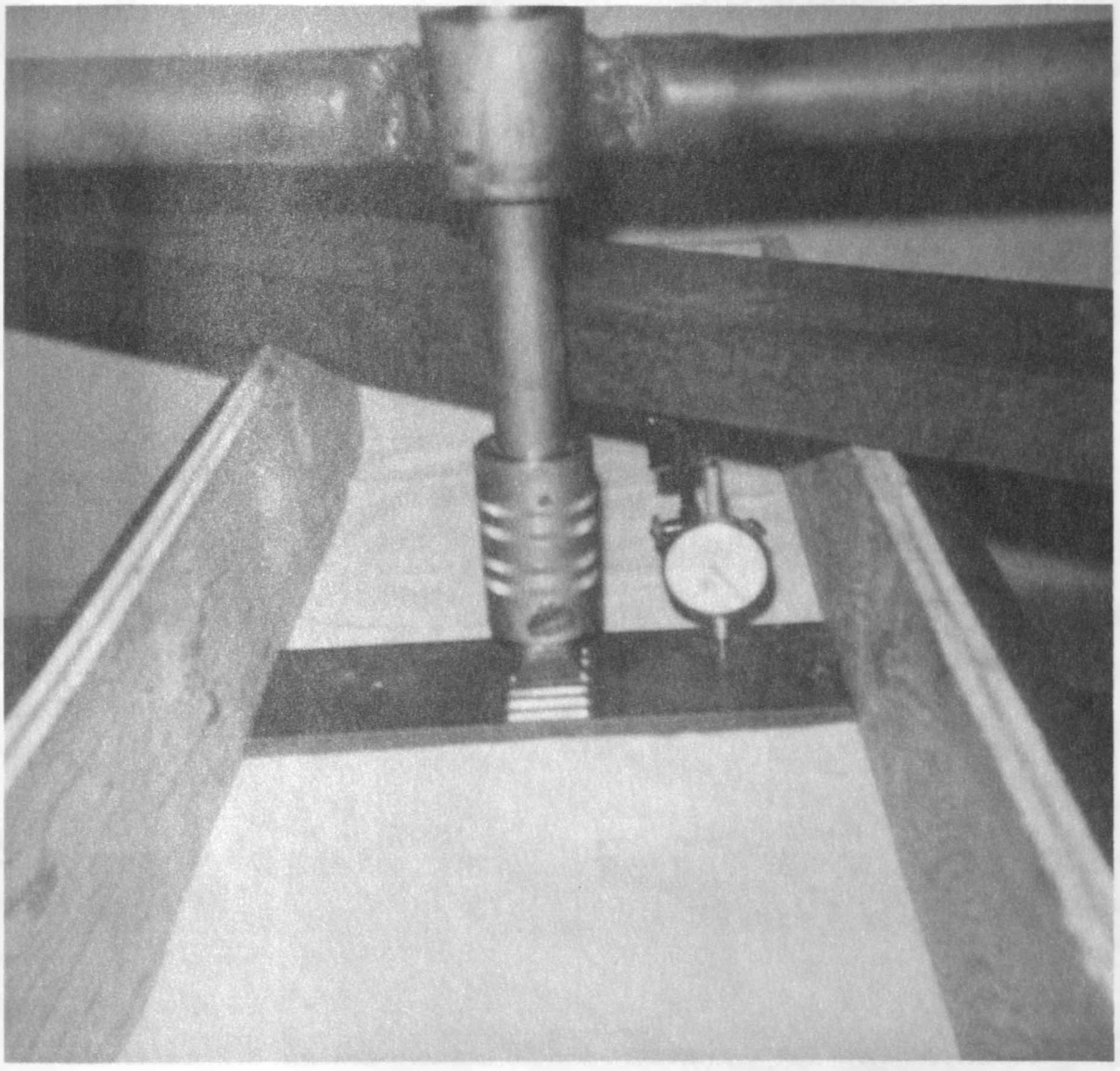

Fig. 3.4 Measuring of footing settlement with micrometer.

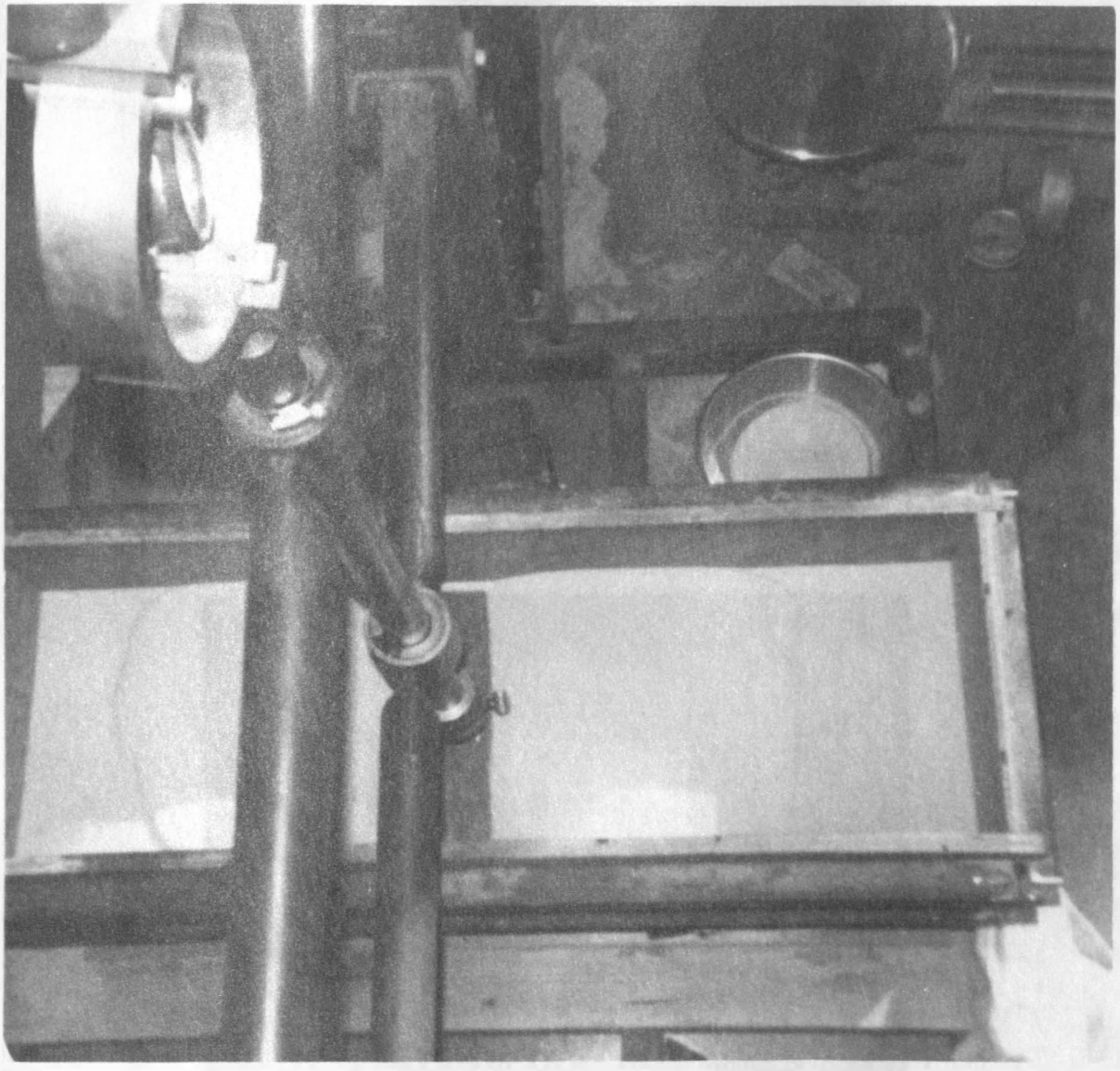

Fig. 3.5 Typical failure pattern for concentric loaded footing.

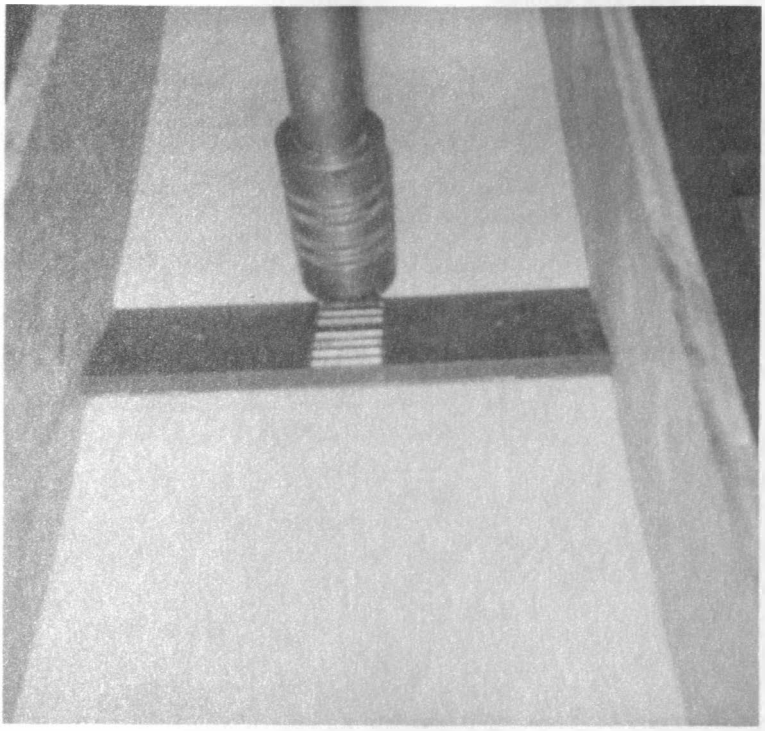

Fig. 3.6 Loss of contact between footing and soil for large eccentricity.

Fig. 3.7 Typical failure pattern for eccentrically loaded footing.

(Figure 3.6). After each test was run the sand was completely taken out of the box, and then put back in and recompacted for the next test.

CHAPTER IV

MODEL TEST RESULTS AND ANALYSIS

4.1 Evaluation of experimental ultimate bearing capacity

As was mentioned in the preceeding chapter, a load was applied to the footing until the maximum load was reached. This load "Q", was recorded for every .01 inches of settlement. From these values of "Q", the load per unit area "q", can be calculated from the following formula:

$$q = \frac{Q}{2BL} \qquad (4.1)$$

where, Q = load applied in pounds

2B = width of the footing in inches

L = length of the footing in inches

These values of q calculated from equation (4.1) were then plotted against the settlement for different values of "e". These plots of q vs. S are shown in Figure (4.1) to Figure (4.5). Figure (4.1) represents a rigid base located at a limited depth. Figure (4.5) represents a rigid base located at a great depth.

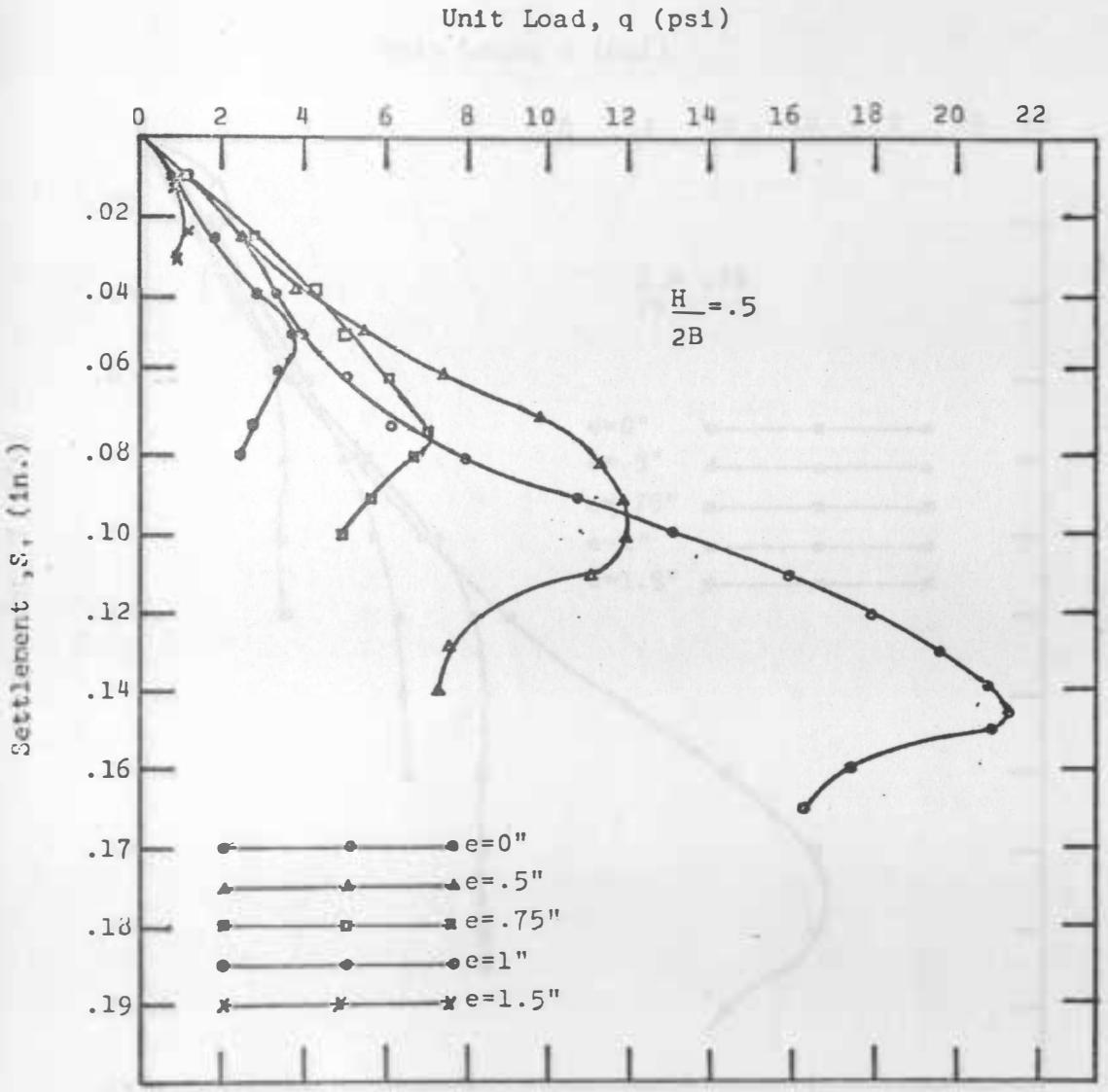

Figure 4.1 q vs. S plot

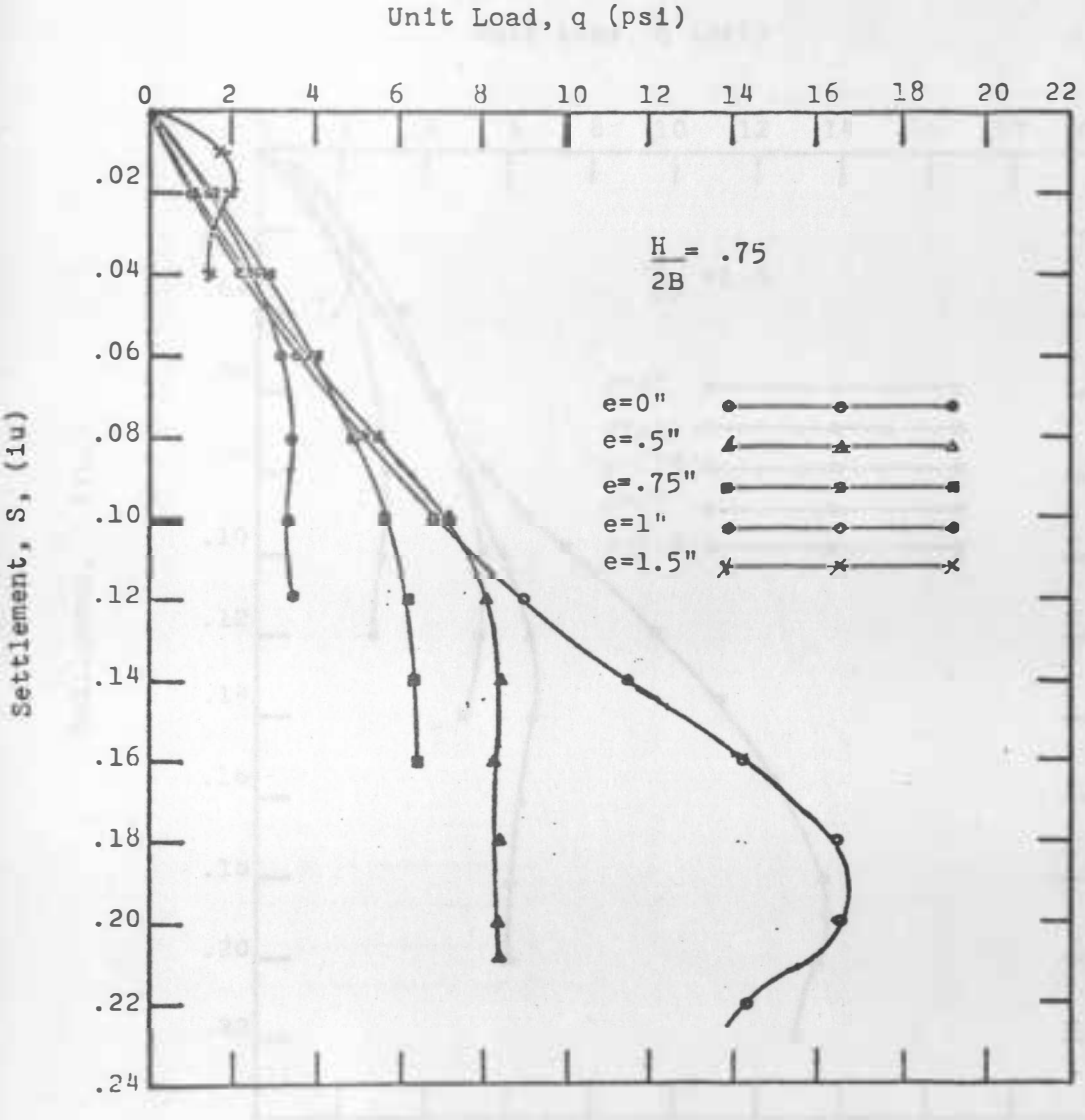

Figure 4.2 q vs. S plot

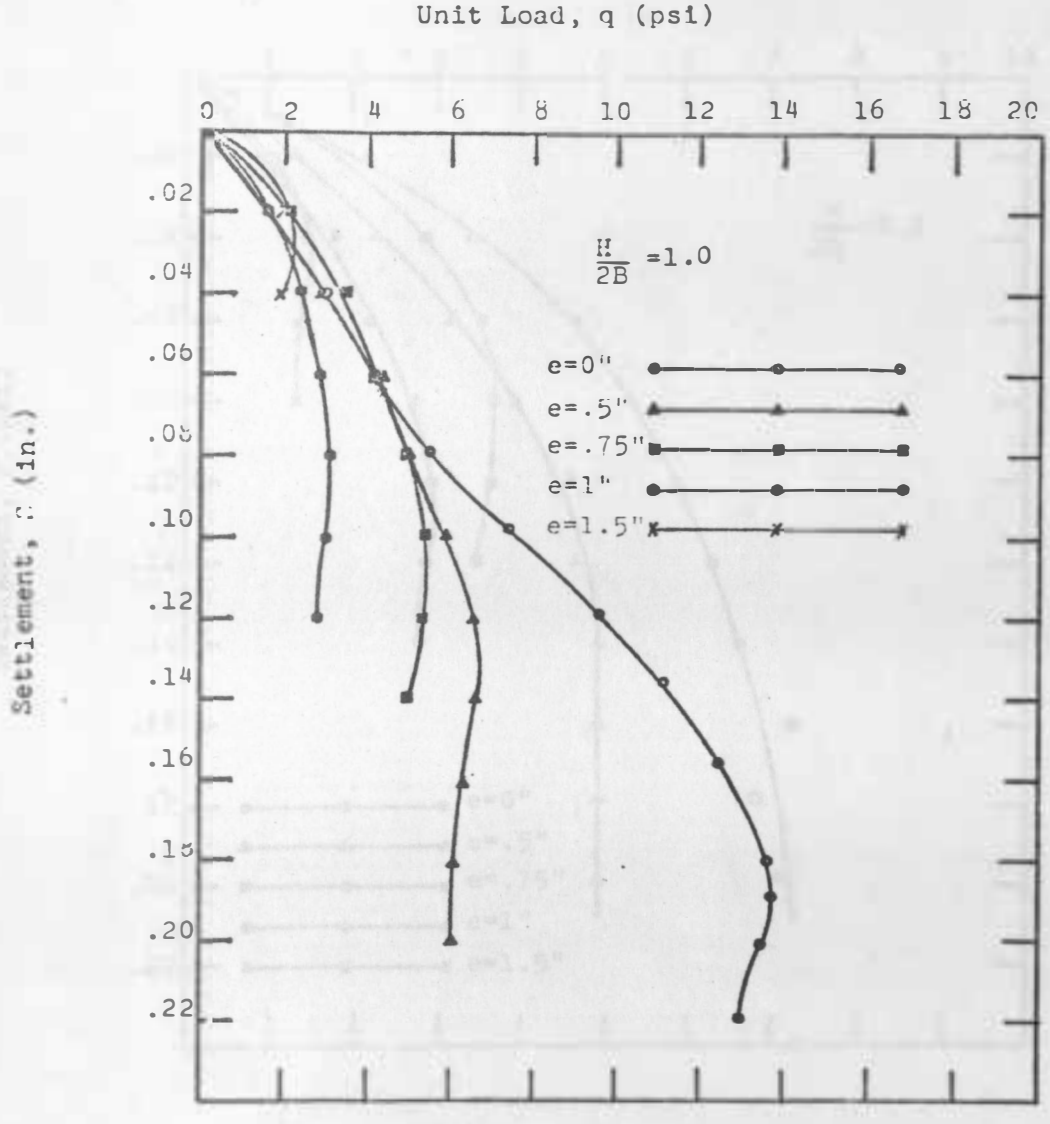

Figure 4.3 q vs. S plot

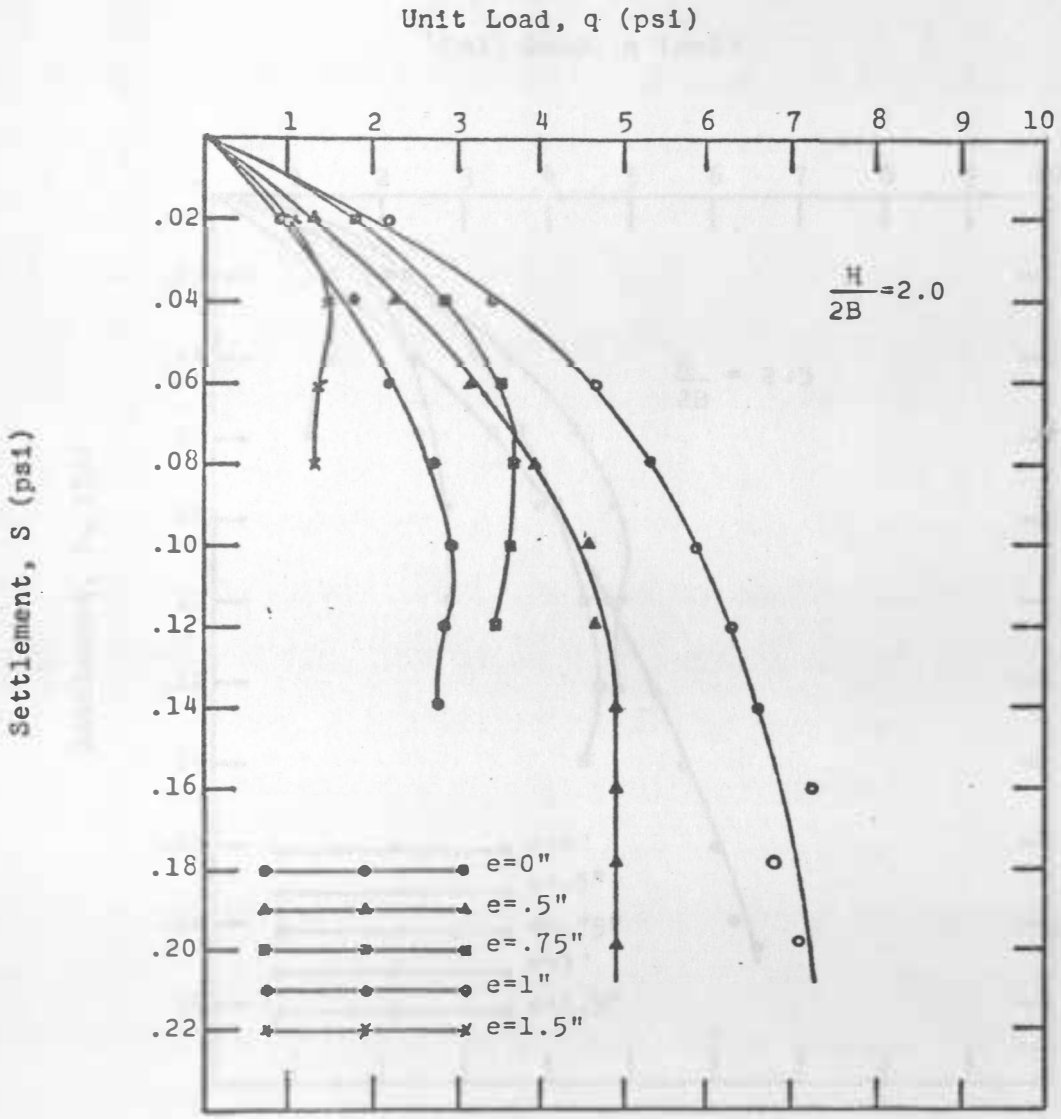

Figure 4.4 q vs. S plot

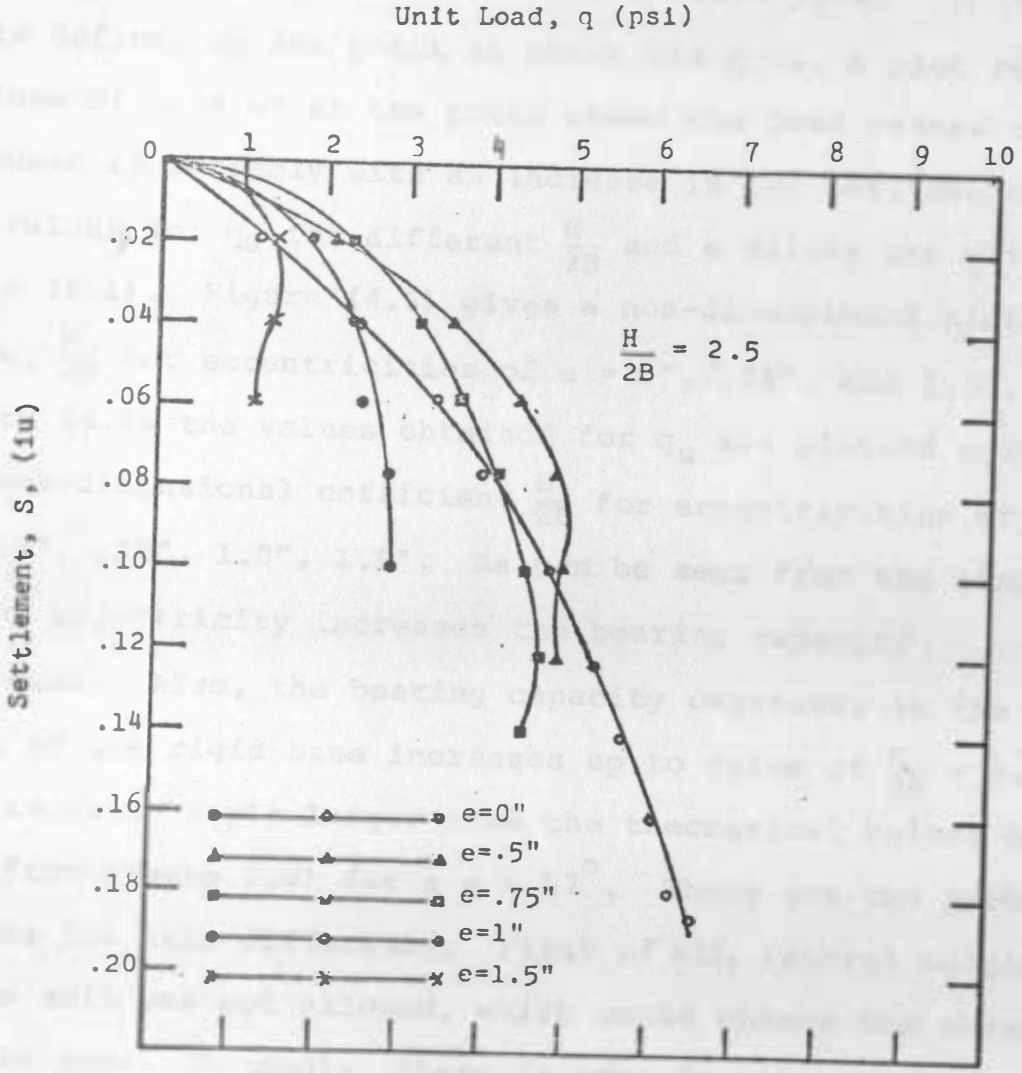

Figure 4.5 q vs. S plot

The value of the ultimate bearing capacity q_u, can be deduced from an examination of the q vs. S plot. The value q_u is defined as the point at which the q vs. S plot reaches a slope of zero or at the point where the load ceases to increase appreciably with an increase in the settlement. The values for q_u for different $\frac{H}{2B}$ and e values are given in Table (4.1). Figure (4.6) gives a non-dimensional plot of $\frac{S}{2B}$ vs. $\frac{H}{2B}$ for eccentricities of e = 0", .75", and 1.5". In Figure (4.7) the values obtained for q_u are plotted against the non-dimensional cofficient $\frac{H}{2B}$ for eccentricities of 0", .5", .75", 1.0", 1.5". As can be seen from the graph, as the eccentricity increases the bearing capacity decreases. Also, the bearing capacity decreases as the depth of the rigid base increases up to value of $\frac{H}{2B}$ = 2.25. This is quite a bit larger than the theoretical values of 1.1 (from Figure 2.8) for a $\phi = 37^{o}$. There are two probable reasons for this difference. First of all, lateral bulging of the soil was not allowed, which could change the shear pattern some. Secondly, there is some friction between the side of the box and the sand grains as the footing is loaded and settlement occurs. This side friction is not taken in to account in the determination of the depth of the slip surfaces. The theoretical determinations depend only on the angle of internal friction, ϕ.

TABLE 4.1

EXPERIMENTAL VALUES

Eccentricity	Soil Depth	$\frac{H}{2B}$	$\frac{H}{2B}$	q_u (psi)	$\frac{q_u}{\gamma B}$	$\frac{q_u}{(1-\frac{2e}{2B})^2 \gamma B}$
0"	2	.50	.50	21.35	176.91	176.91
0"	3	.75	.75	16.92	140.20	140.20
0"	4	1.00	1.00	13.75	113.93	113.93
0"	6	1.50	1.50	9.22	76.40	76.40
0"	8	2.00	2.00	7.29	60.41	60.41
0"	10	2.50	2.50	6.77	56.10	56.10
0"	14	3.50	3.50	6.00	49.72	49.72
.50"	2	.50	.67	11.98	99.27	177.48
.50"	3	.75	1.00	8.20	67.95	121.48
.50"	6	1.00	1.33	6.77	56.10	100.30
.50"	8	2.00	2.67	4.92	40.77	72.89
.50"	10	2.50	3.33	4.91	40.69	72.74
.50"	14	3.50	4.67	4.83	40.02	71.56

TABLE 4.1 (cont.)

Eccentricity	Soil Depth	$\frac{H}{2B}$	$\frac{H}{2B}$	q_u (psi)	$\frac{q_u}{\gamma B}$	$\frac{q_u}{(1-\frac{2e}{2B})^2 \gamma B}$
.75"	2	.50	.80	7.02	58.17	150.32
.75"	3	.75	1.20	6.30	52.20	134.90
.75"	4	1.00	1.60	5.50	54.57	117.77
.75"	6	1.50	2.40	4.43	36.71	94.86
.75"	8	2.00	3.20	3.63	30.08	77.73
.75"	10	2.50	4.00	4.71	39.03	100.86
.75"	14	3.50	5.60	3.92	32.48	83.94
1.00"	2	.50	1.00	3.92	32.56	131.00
1.00"	3	.75	1.50	3.65	30.24	121.67
1.00"	4	1.00	2.00	3.93	32.56	131.00
1.00"	6	1.50	3.00	2.89	32.95	96.33
1.00"	8	2.00	4.00	2.97	24.61	99.00
1.00"	10	2.50	5.00	2.88	23.86	96.00
1.00"	14	3.50	7.00	2.81	23.28	93.67

TABLE 4.1 (cont.)

Eccentricity	Soil Depth	$\frac{H}{2B}$	$\frac{H}{2B}$	q_u (psi)	$\frac{q_u}{\gamma B}$	$\frac{q_u}{(1-\frac{2e}{2B})^2 \gamma B}$
1.50"	2	.50	2.00	1.19	9.86	158.67
1.50"	3	.75	3.00	2.08	17.24	277.33
1.50"	4	1.00	4.00	2.26	18.73	301.33
1.50"	6	1.50	6.00	1.83	15.16	244.00
1.50"	8	2.00	8.00	1.46	12.10	194.67
1.50"	10	2.50	10.00	1.45	12.01	193.33
1.50"	14	3.50	14.00	1.43	11.85	190.67

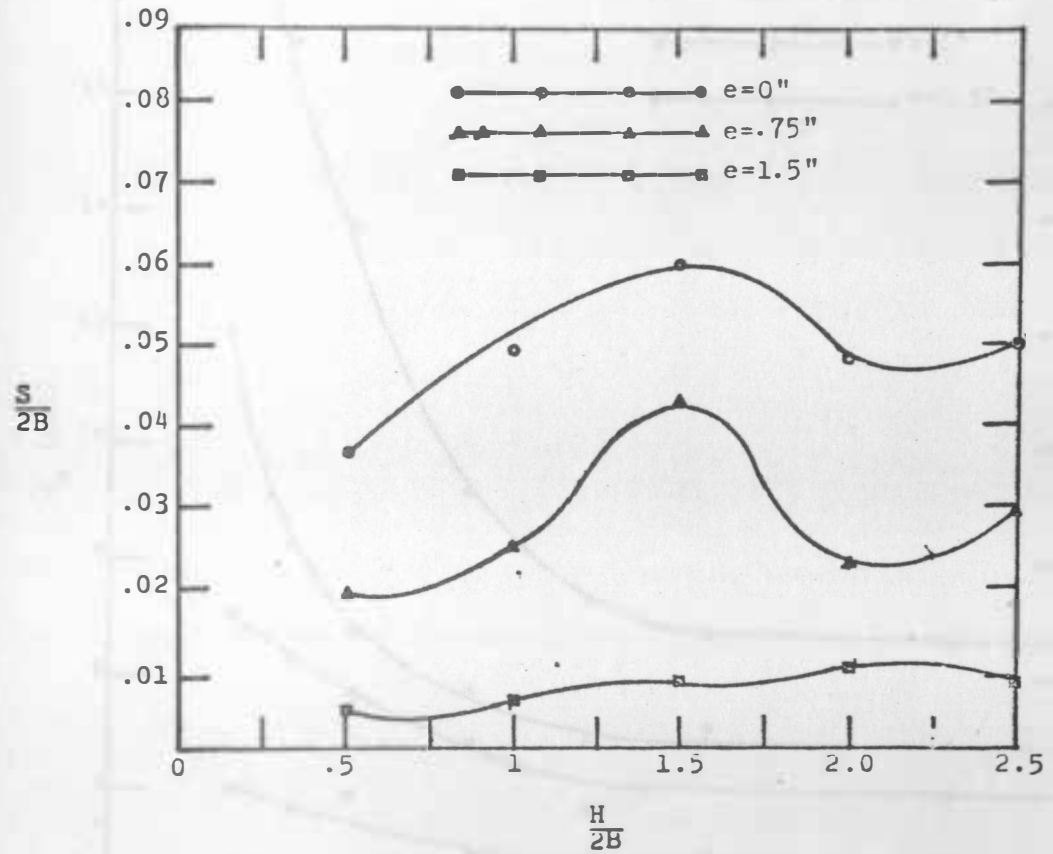

Figure 4.6 Non dimensional plot of $\frac{S}{2B}$ vs. $\frac{H}{2B}$ for e = 0", .75", 1.5"

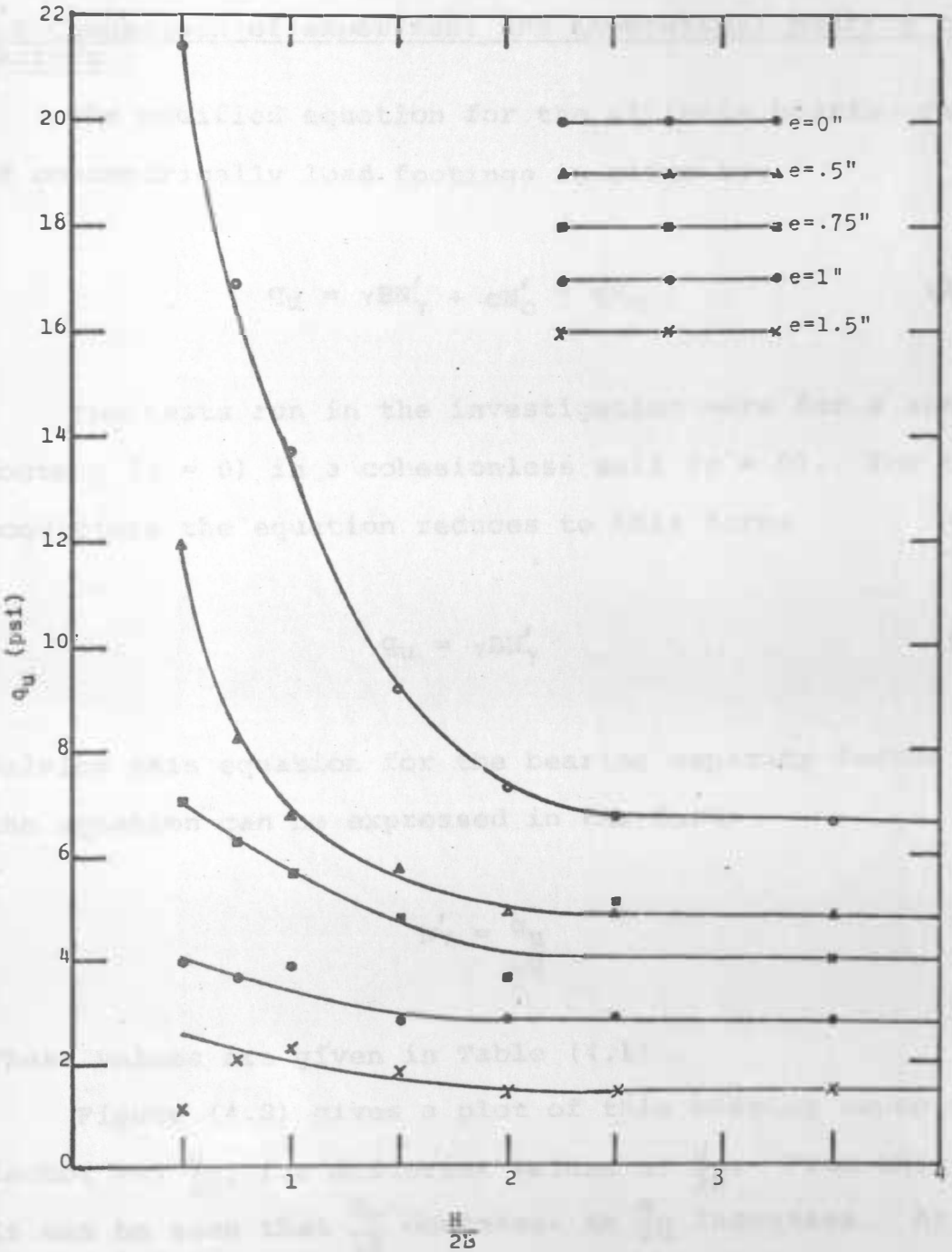

Figure 4.7 Plot of q_u vs. $\frac{H}{2B}$ for e = 0", .5", .75", 1.0", 1.5"

4.2 Comparison of experiment and theoretical bearing capacity factors

The modified equation for the ultimate bearing capacity of concentrically load footings is given by:

$$q_u = \gamma B N'_\gamma + c N'_c + q N'_q \qquad (2.17)$$

The tests run in the investigation were for a surface footing (q = 0) in a cohesionless soil (c = 0). For these conditions the equation reduces to this form:

$$q_u = \gamma B N'_\gamma \qquad (4.2)$$

Solving this equation for the bearing capacity factor N'_γ, the equation can be expressed in the form:

$$N'_\gamma = \frac{q_u}{\gamma B} \qquad (4.3)$$

These values are given in Table (4.1).

Figure (4.3) gives a plot of this bearing capacity factor vs. $\frac{e}{2B}$, for different values of $\frac{H}{2B}$. From this graph it can be seen that $\frac{q_u}{\gamma B}$ decreases as $\frac{e}{2B}$ increases. At a value of $\frac{e}{2B}$ = .5, the bearing capacity factor is equal to zero. Also from this graph it can be seen that as the

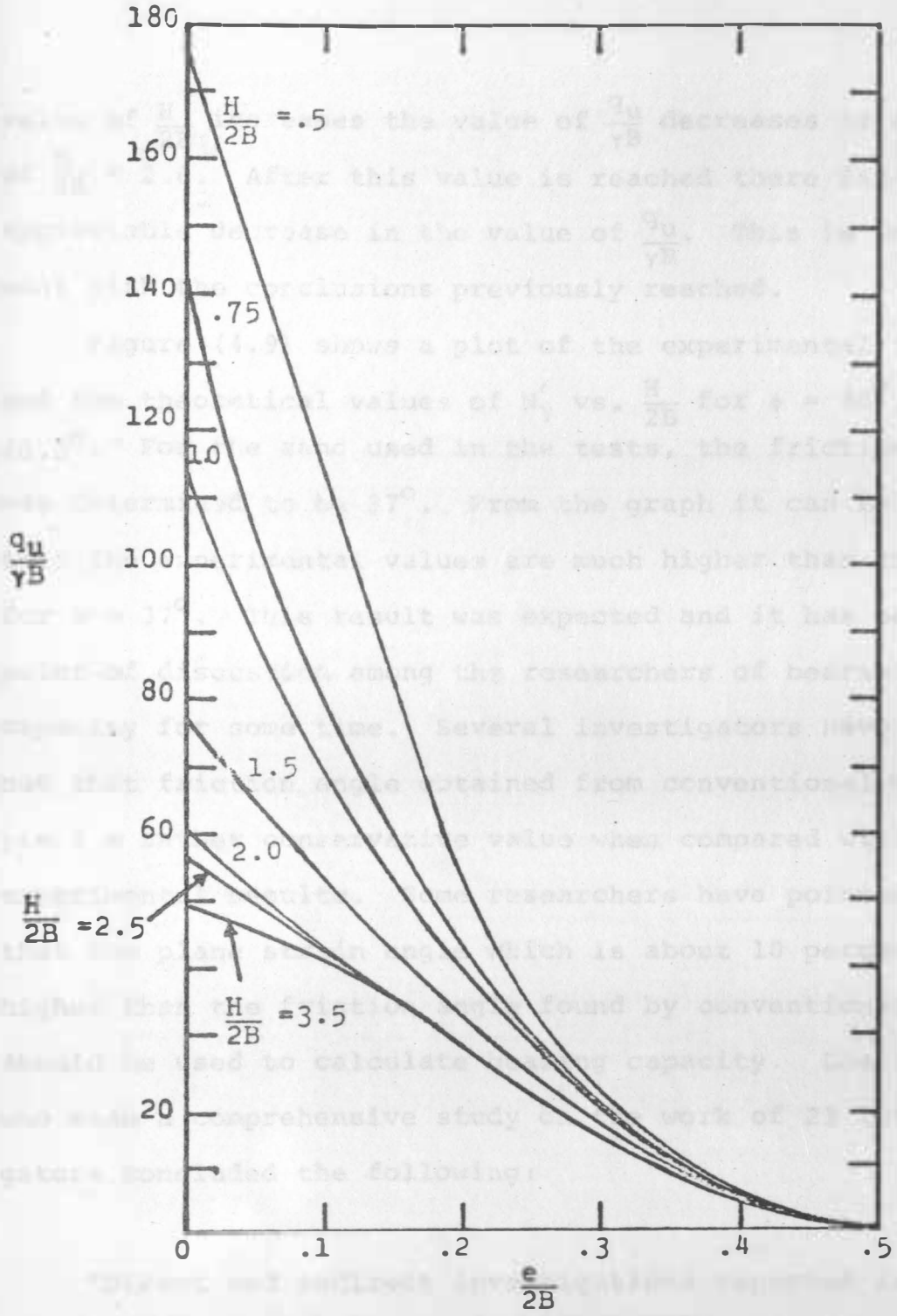

Figure 4.8 Non-dimensional plot of $\frac{q_u}{\gamma B}$ vs. $\frac{e}{2B}$

value of $\frac{H}{2B}$ increases the value of $\frac{q_u}{\gamma B}$ decreases to a value of $\frac{H}{2B} \simeq 2.0$. After this value is reached there isn't any appreciable decrease in the value of $\frac{q_u}{\gamma B}$. This is in agreement with the conclusions previously reached.

Figure (4.9) shows a plot of the experimental (e = 0) and the theoretical values of N'_γ vs. $\frac{H}{2B}$ for $\phi = 36^o$, 39^o, 40.5^o. For the sand used in the tests, the friction angle was determined to be 37^o. From the graph it can be seen that the experimental values are much higher than those for $\phi = 37^o$. This result was expected and it has been a point of discussion among the researchers of bearing capacity for some time. Several investigators have pointed out that friction angle obtained from conventional tests yield a rather conservative value when compared with experimental results. Some researchers have pointed out that the plane strain angle which is about 10 percent higher than the friction angle found by conventional methods should be used to calculate bearing capacity. Lee (1970) who made a comprehensive study on the work of 23 investigators concluded the following:

> "Direct and indirect investigations reported in the literature agree with the results of this study that under drained conditions that plane strain angle of internal friction exceeds the

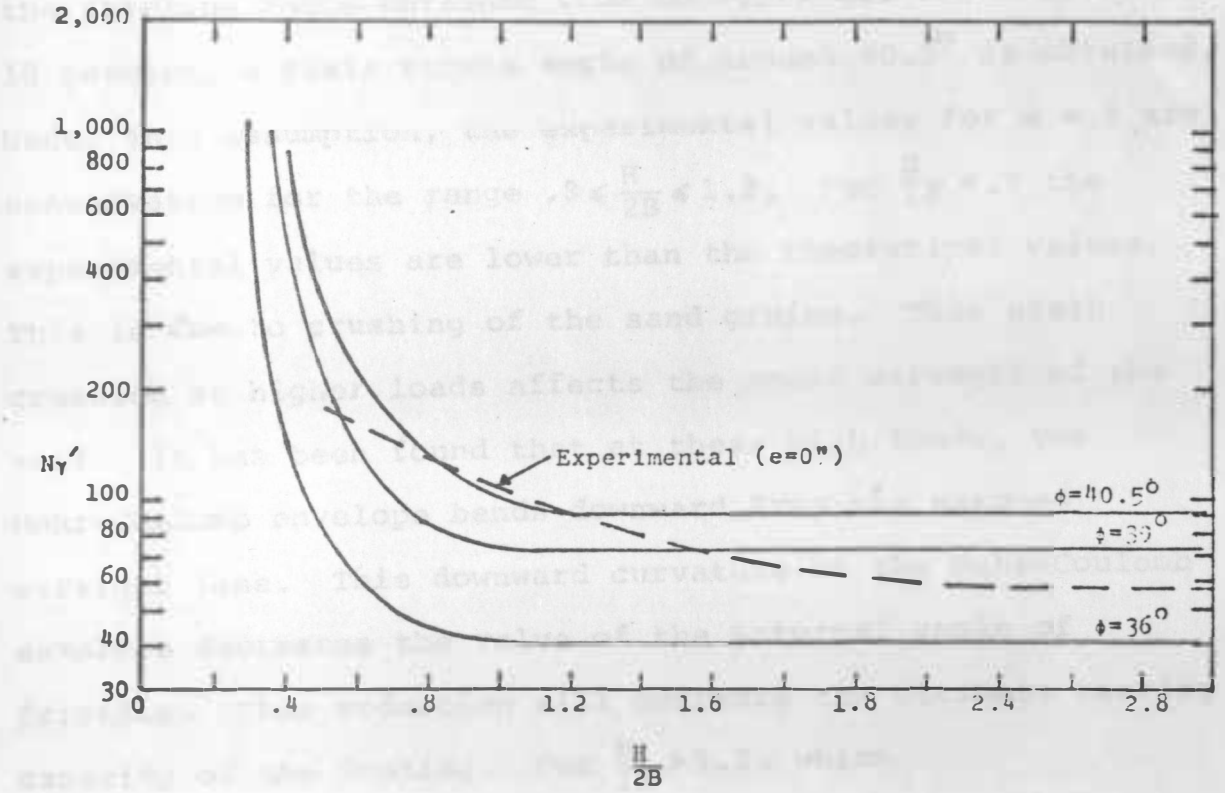

Figure 4.9 Comparison of theoretical and experimental values for N_γ vs. $\frac{H}{2B}$ for e = 0"

value obtained from trixial tests by 0^{o} to about 6^{o} or 8^{o}. The greatest difference is associated with dense sands at low confining pressures, . . ."

Using this assumption that the plane strain angle exceeds the friction angle obtained from conventional tests by about 10 percent, a plain strain angle of around 40.5^{o} is obtained. Under this assumption, the experimental values for e = 0 are conservative for the range $.8 \leq \frac{H}{2B} \leq 1.2$. For $\frac{H}{2B} < .8$ the experimental values are lower than the theoretical values. This is due to crushing of the sand grains. This grain crushing at higher loads affects the shear strength of the soil. It has been found that at these high loads, the Mohr-Coulomb envelope bends downward from the assumed straight line. This downward curvature of the Mohr-Coulomb envelope decreases the value of the internal angle of friction. This reduction will decrease the ultimate bearing capacity of the footing. For $\frac{H}{2B} > 1.2$, which rigid base located at a great depth, the theoretical values are on the conservative side of the experimental values. The general nature of the experimental N'_{γ} is the same as that found by Meyerhof (1974).

As mentioned previously, if an eccentric load is applied, the effective width of the footing is reduced by (2B - 2e). Using this assumption, Jumikis (1956) expressed the general bearing capacity equation in the form:

$$q_u = (1 - \frac{2e}{2B})(cN'_c + qN'_q) + (1 - \frac{2e}{2B})^2 \gamma B N'_\gamma \qquad (2.24)$$

As before, the tests were run on a surface footing (q = 0) with a cohesionless sand (c = 0). Therefore the above equation reduces to

$$q_u = (1 - \frac{2e}{2B})^2 \gamma B N'_\gamma \qquad (4.5)$$

These values are given in Table (4.1). The value of $\frac{q_u}{(1-\frac{2e}{2B})^2 \gamma B}$ vs. $\frac{H}{2B}$, is plotted in Figure (4.10) and Figure (4.11) for e = .5", .75", 1.0", and 1.5". Again the values of N'_γ are plotted for friction angles of 36^o, 39^o, and 40.5^o for comparison. As can be seen from the graphs, the plane strain angle theory holds true for the case of eccentrically loaded footings. Applying Meyerhof's theory for eccentrically loaded footings, it can be seen that the results are in fairly good agreement with the theoretical values. The experimental values tend to be conservative in the range

where shallow conditions for the rigid base occur, becoming less conservative as the depth to the rigid base increases. It can also be seen that as the eccentricity increases, the experimental values as given by Meyerhof's theory, become more and more conservative. At e = 1.50" the experimental values as given by Meyerhof's theory are = 100% greater than those given to the theory. The reason for this is probably the loss of contact of the footing with the soil (Figure 3.6).

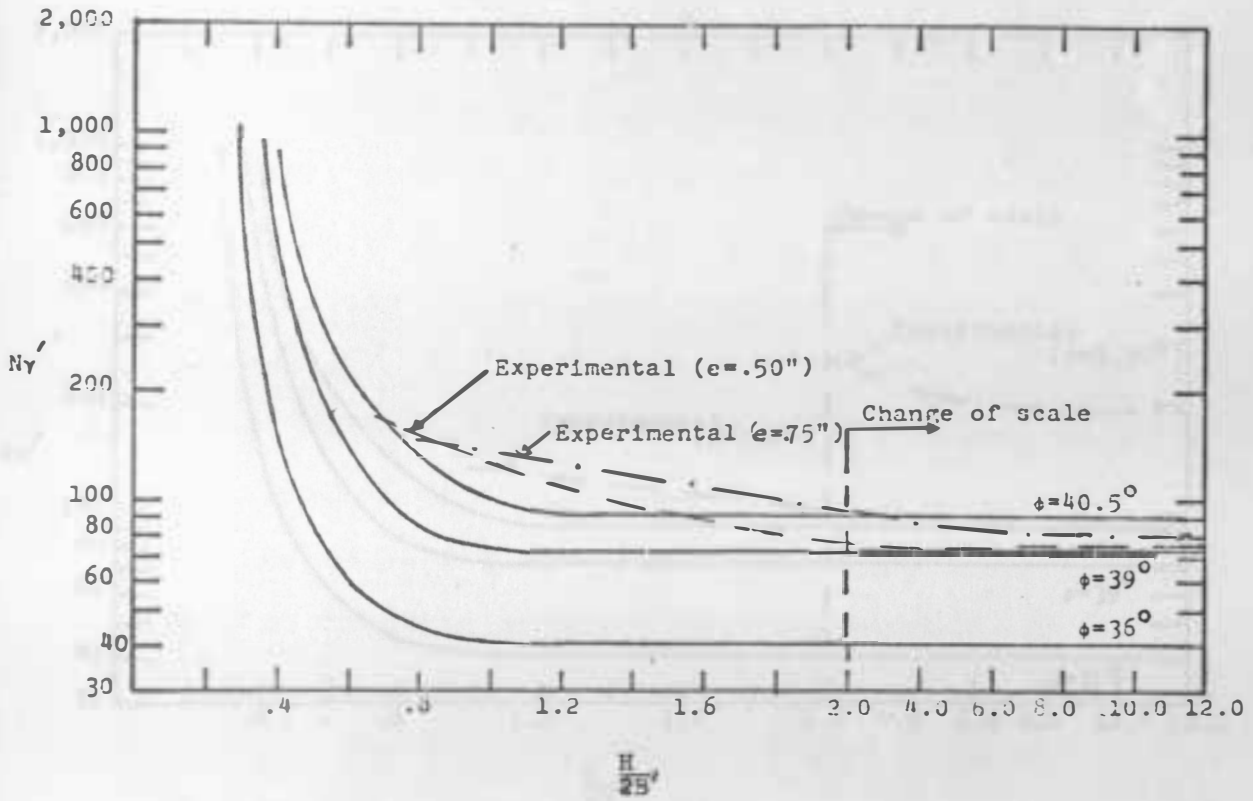

Figure 4.10 Comparison of theoretical and experimental values for N_γ' vs. $\frac{H}{2B'}$ for e = .50", .75".

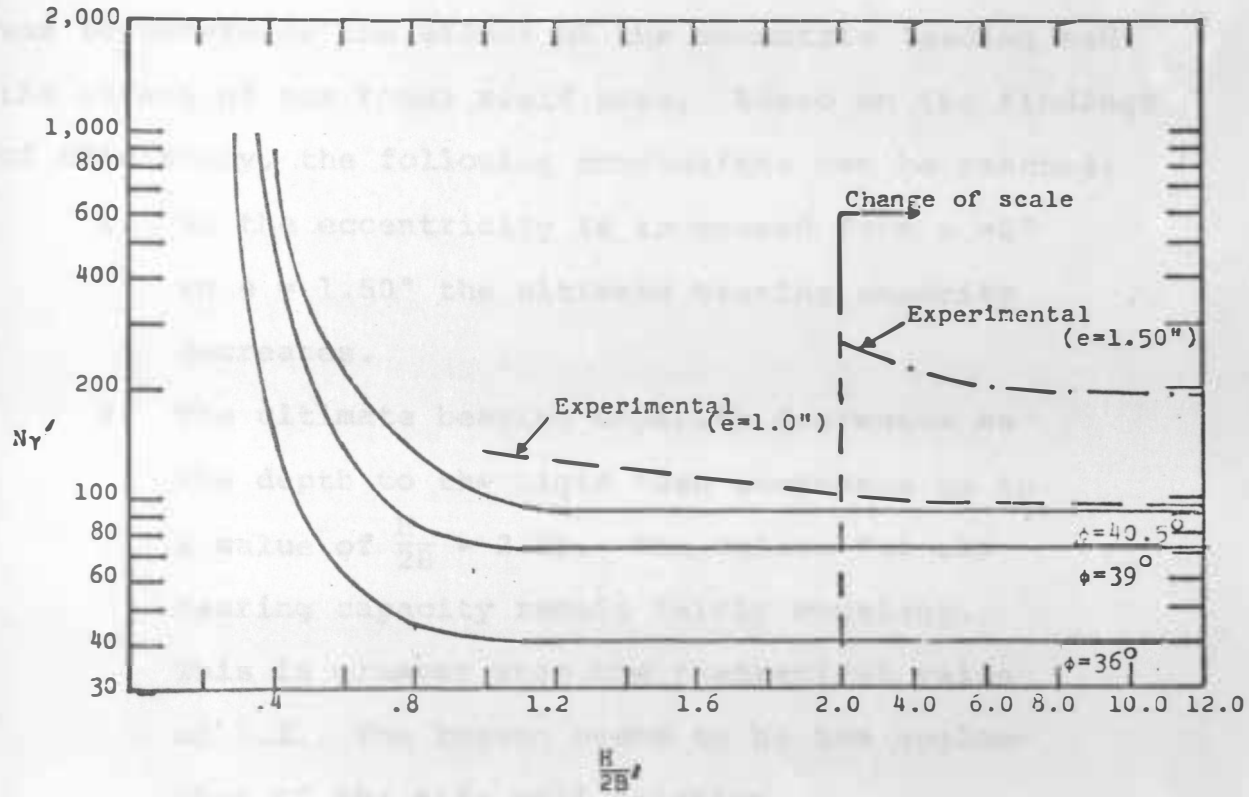

Figure 4.11 Comparison of theoretical and experimental values for N_γ' vs. $\frac{H}{2B'}$ for e = 1.0", 1.5"

CHAPTER V

CONCLUSION

Tests were run in the laboratory on concentrically and eccentricially loaded strip footings, with a rough rigid base located at varing depths. The purpose of these tests was to determine the effect of the eccentric loading and the effect of the rough rigid base. Based on the findings of this study, the following conclusions can be reached:

1. As the eccentricity is increased from e =0" to e = 1.50" the ultimate bearing capacity decreases.
2. The ultimate bearing capacity decreases as the depth to the rigid base increases up to a value of $\frac{H}{2B} = 2.25$. The values for the bearing capacity remain fairly constant. This is greater than the theoretical value of 1.1. The reason seems to be the neglection of the side wall friction.
3. The experimental values obtained are in close agreement with the values given for $\phi = 40.5^{o}$ although the friction angle for the sand used in the tests run = 37^{o}.

4. For the concentrically load footings for $\frac{H}{2B} < .8$ the theoretical values for $\frac{q_u}{\gamma B}$ give a conservative estimate.
5. For $.8 \leq \frac{H}{2B} \leq 1.2$ the experimental values for N'_γ are on the conservative side of the theoretical values.
6. For great depth conditions, the theoretical values given for N'_γ are on the conservative side of the theoretical values.
7. By applying Meyerhof's theory for eccentrically loaded footings, the results give the same type of trend as those for the concentrically loaded footing. This is the same conclusion as reached by various investigators.
8. As the eccentricity is increased, the experimental values become more and more conservative for N'_γ.
9. Based on the results of this experiment, Meyerhof's theory for eccetrically loaded footings holds true except for footings loaded with large eccentricities.

10. For footings loaded with large eccentricities the theoretical values greatly under estimate N'_γ. Therefore, if footings have to be loaded with an eccentric load, this eccentricity should be kept as small as possible.

APPENDIX I

Conversion to S.I. Units

1 ft. = .305 m
1 in. = 25.4 mm
1 lb. = .454 kg
1 lb. = 4.48 N
1 psf = 47.9 N/m^2
1 psi = 6.89 kN/m^2
1 pcf = .158 kN/m^3

BIBLIOGRAPHY

Caquot, A., and J. Kerisel. "Ultimate Bearing Capacity of a Foundation Lying on the Surface of a Cohesionless Soil." Proceedings, Third International Conference on Soil Mechanics and Foundation.

DeBeer, E.E., and A. Vesic. "Etude experimentale de la capacite portante du sable sous des foundations directes establies en surface." Annales des Travaux Publics de Belgique, Vol. 59, No. 3, 1958.

Jumikis, A.R. "Rupture Surfaces in Sand Under Oblique Loads." Journal of the Soil Mechanics and Foundations Division, ASCE, Vol. 82, No. SM3, Proc. Paper 861, July, 1956.

Ko, H.Y., and L.W. Davidson. "Bearing Capacity of Footings in Plane Strain. Journal of the Soil Mechanics and Foundations Division, ASCE, Vol. 99, No. SM1, Proc. Paper 9496, 1973.

Lambe, T.W., and R.V. Whitman. Soil Mechanics. New York, N.Y.: John Wiley and Sons, Inc., 1969.

Lee, K.L. "Comparison of Plane Strain and Triaxial Tests on Sand." Journal of the Soil Mechanics and Foundations Division, ASCE, Vol. 96, No. SM3, Proc. Paper 7276, 1970.

Lundgren, H., and K. Mortensen. "Determination by the Theory of Plasticity of the Bearing Capacity of Continuous Footings on Sand." Proceedings, Third International Conference on Soil Mechanics and Foundation Engineering, Vol. I. Zurich, Switerzerland, 1953.

Mandel, J., and J. Salencon. "Force portante d'un sol une assise. rigide." Proceedings, Seventh International Conference on Soil Mechanics and Foundation Engineering, Vol. 2. Mexico City, Mexico, 1969.

Meyerhof, G.G. "The Bearing Capacity of Foundation Under Eccentric and Inclined Load." Proceedings, Third International Conference on Soil Mechanics and Foundation Engineering, Vol. I. Zurich, Switzerland, 1953.

Meyerhof, G.G. "Some Recent Research on the Bearing Capacity of Foundations." Canadian Geotechnical Journal, Vol. I, No. 1, 1963.

Meyerhof, G.G. "Ultimate Bearing Capacity of Footings on Sand Layer Overlying Clay." Canadian Geotechnical Journal, Vol. II, No. 2, 1974.

Prakash, S., and S. Saran. "Bearing Capacity of Eccentrically Loaded Footings " Journal of the Soil Mechanics and Foundations Division, ASCE, Vol. 97, No. SM1, Proc. Paper 7814, 1971.

Prandlt, L. "Uber die Endringungsfestigkeit plastisher Baustoffe und die Festigkeit von Schneiden." Zeitschrift fur Angewandtle Mathematik und Mechanik, Vol. 1, No. 1. Basel, Switerzerland, 1921.

Reissner, H. "Zum Erddruckproblem." Proceedings, First International Conference on Applied Mechanics. Delft, The Netherlands, 1924.

Terzaghi, K. Theoretical Soil Mechanics. New York, N.Y.: John Wiley and Sons, Inc., 1943.

Vesic, A.S. "Analysis of Ultimate Loads of Shallow Foundations." Journal of the Soil Mechanics and Foundations Division, ASCE, Vol. 99, No. SM1, 1973.